



**MARMARA UNIVERSITY  
FACULTY OF ENGINEERING**



**U AND V BENDING ANALYSIS WITH PRESS  
BRAKE**

---

MUHAMMED MUSTAFA ALBAYRAK  
ALAATTİN EFE TOPUZ  
SALİH TANER SEZGİN

**GRADUATION PROJECT REPORT**  
Department of Mechanical Engineering

**Supervisor**  
Prof. Dr. Aykut KENTLİ

**ISTANBUL, 2025**

---



**MARMARA UNIVERSITY  
FACULTY OF ENGINEERING**



**U And V Bending Analysis with Press Brake  
by**

**Muhammed Mustafa Albayrak, Alaattin Efe Topuz, Salih Taner Sezgin**

**June 23, 2025, Istanbul**

**SUBMITTED TO THE DEPARTMENT OF MECHANICAL ENGINEERING IN  
PARTIAL FULFILLMENT OF THE REQUIREMENTS FOR THE DEGREE**

**OF**

**BACHELOR OF SCIENCE**

**AT**

**MARMARA UNIVERSITY**

The author(s) hereby grant(s) to Marmara University permission to reproduce and to distribute publicly paper and electronic copies of this document in whole or in part and declare that the prepared document does not in anyway include copying of previous work on the subject or the use of ideas, concepts, words, or structures regarding the subject without appropriate acknowledgement of the source material.

Signature of Author(s) .....  
Department of Mechanical Engineering

Certified By .....  
Project Supervisor, Department of Mechanical Engineering

Accepted By .....  
Head of the Department of Mechanical Engineering

## **ACKNOWLEDGEMENT**

First of all, we would like to thank our supervisor Prof. Dr. Aykut Kentli for the valuable guidance and advice on preparing this thesis and giving us moral and material support. We also would like to thank Enta Technical Automation Industry Mechanical Engineering Co. Ltd. for their support in the manufacturing of the machine.

January, 2025

Muhammed Mustafa Albayrak  
Alaattin Efe Topuz  
Salih Taner Sezgin

# CONTENTS

|   |    |
|---|----|
| <b>ABSTRACT .....</b>   | 6  |
| <b>SYMBOLS .....</b>  | 7  |
| <b>ABBREVIATIONS .....</b>  | 8  |
| <b>LIST OF FIGURES .....</b>  | 9  |
| <b>LIST OF TABLES .....</b>   | 10 |
| <b>1. INTRODUCTION.....</b>   | 11 |
| <b>2. LITERATURE REVIEW.....</b>  | 14 |
| <b>2.1. Bending.....</b>  | 14 |
| <b>2.1.1. Definition and Terminology .....</b>                                    | 14 |
| <b>2.1.2. Moment of Bending .....</b>   | 16 |
| <b>2.1.3. Types of Bending Operations .....</b>                                   | 18 |
| <b>2.2. Springback .....</b>  | 20 |
| <b>2.3. Advantages and Disadvantages of Bending Process .....</b>                 | 23 |
| <b>2.4. Press Brake Process .....</b>   | 25 |
| <b>2.4.1. Origin and Industrial Significance of The Press Brake Process .....</b> | 26 |
| <b>3. HANDEMADE PRESS BRAKE MACHINE SETUP .....</b>                               | 27 |
| <b>3.1. Parts of Hand Made Press Brake.....</b>                                   | 28 |
| <b>3.1.1. Upper Die (Punch).....</b>  | 28 |
| <b>3.1.2. Lower Die (Base Die Block).....</b>                                     | 29 |
| <b>3.1.3 Rack and Pinion Mechanism.....</b>                                       | 29 |
| <b>3.1.4. Manual Handle (Crank Arm) .....</b>                                     | 29 |
| <b>3.1.5. Support Column and Machine Base.....</b>                                | 30 |
| <b>3.1.6 Adjustable Back Gauge .....</b>  | 30 |
| <b>3.2. Materials .....</b>   | 31 |
| <b>3.2.1 UNS C17200 Copper Alloy .....</b>  | 31 |
| <b>3.2.2 AISI 4140 Steel .....</b>  | 32 |
| <b>3.4. Calculations .....</b>  | 33 |
| <b>3.4.1. Gear .....</b>  | 33 |
| <b>3.4.2. Sheet Metal.....</b>  | 46 |
| <b>3.4.3. Buckling .....</b>  | 51 |
| <b>3.4.4. Shaft.....</b>  | 56 |
| <b>4. SIMULATION SETUP.....</b>   | 59 |
| <b>4.1. Geometry and Modeling .....</b>   | 59 |
| <b>4.2. Simulation and Results .....</b>  | 61 |

|  |           |
|--|-----------|
| 4.2.1. U-Bending Analysis – Step 1 ..... | 61        |
| 4.2.2. U Bending – Step 2 .....          | 69        |
| 4.2.3. V-Bending Analysis .....          | 72        |
| 4.3 General Evaluation .....             | 75        |
| <b>5. RESULTS &amp; DISCUSSION.....</b>  | <b>76</b> |
| <b>6. CONCLUSION.....</b>                | <b>77</b> |
| <b>7. REFERENCES .....</b>               | <b>79</b> |

## **ABSTRACT**

In this study, a manually operated mini press brake was designed for use in small-scale production environments, maintenance-repair workshops, and educational laboratories. The developed device operates solely through a differential gear and lever mechanism, without the need for CNC systems, hydraulic pumps, or heavy steel frameworks. These features make it a compact, economical, and portable solution.

During the design phase, essential engineering processes were carried out, including material selection, static strength calculations, gear contact analysis, and ergonomic optimization of lever lengths. These analyses were conducted to ensure both the durability and user-friendliness of the device.

In the manufacturing phase, shafts, gears, and lever components were machined using CNC equipment and assembled through TIG welding. All surfaces were treated with a protective matte chromate coating. In addition, a quick-change die system was integrated, allowing the upper and lower dies to be replaced in less than 30 seconds.

Experimental tests performed on the prototype yielded consistent bending results within a  $\pm 2^\circ$  angular tolerance. Simulation studies were carried out using ANSYS Workbench software to analyze the stresses, deformations, and plastic strain distributions occurring during the bending process in detail. The alignment between numerical data and experimental results confirmed the reliability of the design and validated the engineering approach adopted in this study.

## SYMBOLS

- σ:** Gear bending stress  
**S<sub>F</sub>:** factor of safety  
**σ<sub>C</sub>:** contact stress  
**S<sub>H</sub>:** factor of safety  
**W<sup>t</sup>:** Load  
**d<sub>p</sub>:** Diameter  
**N:** Speed  
**H:** Horsepower  
**T:** Torque  
**F:** Force  
**Φ:** Pressure Angle  
**F<sub>t</sub>:** Tangential force  
**F<sub>r</sub>:** Radial force  
**K<sub>O</sub>:** Overload factor  
**K<sub>V</sub>:** Dynamic factor  
**V:** Pitch line velocity  
**Q<sub>v</sub>:** Quality value ranges  
**K<sub>S</sub>:** Size factor  
**K<sub>H</sub>:** Load factor  
**C<sub>mc</sub>:** Load correction factor  
**C<sub>pf</sub>:** Pinion proportion factor  
**F:** Face Width  
**C<sub>pm</sub>:** Pinion proportion modifier  
**C<sub>ma</sub>:** Mesh alignment factor  
**C<sub>e</sub>:** Mesh alignment correction factor  
**K<sub>B</sub>:** Rim thickness factor  
**h<sub>t</sub>:** Tooth Height  
**m<sub>B</sub>:** Back-up ratio  
**b:** Half width  
**m<sub>t</sub>:** Transverse module  
**Y<sub>J</sub>:** Bending strength geometry factor  
**q:** Number of contact per revolution  
**L:** Life  
**Y<sub>N</sub> and Z<sub>N</sub>:** Stress cycle factor bending stress  
**Y<sub>θ</sub>:** Temperature factor  
**Y<sub>Z</sub>:** Reliability factor  
**Z<sub>E</sub>:** Elastic coefficient  
**Z<sub>R</sub>:** Surface condition factor  
**S<sub>C</sub>:** Allowable contact stress  
**Z<sub>I</sub>:** Surface strength geometry factor  
**m<sub>N</sub>:** Load sharing ratio  
**m<sub>G</sub>:** Speed ratio  
**Z<sub>w</sub>:** Hardness ratio factor  
**(L/k):** Slenderness ratio  
**E:** Elastic modulus  
**M:** Bending moment  
**S<sub>t</sub>:** Allowable bending stress

## ABBREVIATIONS

|               |   |
|---------------|---|
| <b>Al</b>     | Aluminum  |
| <b>ANSYS</b>  | Analysis System (Engineering simulation software)   |
| <b>ASM</b>    | American Society for Metals                         |
| <b>CAD</b>    | Computer-Aided Design                               |
| <b>CAM</b>    | Computer-Aided Manufacturing                        |
| <b>CNC</b>    | Computer Numerical Control                          |
| <b>Cu</b>     | Copper  |
| <b>DoF</b>    | Degree of Freedom                                   |
| <b>Eq.</b>    | Equation  |
| <b>FEA</b>    | Finite Element Analysis                             |
| <b>FEM</b>    | Finite Element Method                               |
| <b>Fig.</b>   | Figure  |
| <b>HAZ</b>    | Heat Affected Zone                                  |
| <b>MRO</b>    | Maintenance, Repair, and Overhaul                   |
| <b>Ni</b>     | Nickel  |
| <b>Ref.</b>   | Reference   |
| <b>SME</b>    | Small and Medium-sized Enterprises                  |
| <b>SPR</b>    | Springback  |
| <b>SS</b>     | Stainless Steel                                     |
| <b>U-bend</b> | U-die bending                                       |
| <b>UTS</b>    | Ultimate Tensile Strength / Ultimate Tensile Stress |
| <b>V-bend</b> | V-die bending                                       |
| <b>YS</b>     | Yield Strength                                      |

.

## LIST OF FIGURES

|   |    |
|---|----|
| <b>Figure 1.</b> Typical examples of sheet metal bend parts. ....                       | 15 |
| <b>Figure 2.</b> Neutral axis of a bended sheet .....                                   | 15 |
| <b>Figure 3.</b> Elasticity, Plasticity and Elastic Limit .....                         | 18 |
| <b>Figure 4.</b> V-Die Bending .....  | 19 |
| <b>Figure 5.</b> U-Die Bending .....  | 20 |
| <b>Figure 6.</b> Elastic Springback .....   | 22 |
| <b>Figure 7.</b> Strain and Stress Behaviour During the Forming Process .....           | 23 |
| <b>Figure 8.</b> Mini Press Brake. ....   | 31 |
| <b>Figure 9.</b> Pitch Diameter of Gear .....   | 34 |
| <b>Figure 10.</b> Forces on the Tooth of Gear .....                                     | 35 |
| <b>Figure 11.</b> Face Width of Gear (F) .....  | 39 |
| <b>Figure 12.</b> Rim Thickness and Tooth Height of Gear .....                          | 40 |
| <b>Figure 13.</b> Spur Gear Geometry Factor .....                                       | 41 |
| <b>Figure 14.</b> Allowable Bending Stress Number for Steel Gear .....                  | 42 |
| <b>Figure 15.</b> Allowable Bending Stress Number for Through Hardened Steel Gears..... | 42 |
| <b>Figure 16.</b> Bending Strength Stress Cycle Factor $Y_N$ .....                      | 43 |
| <b>Figure 17.</b> Elastic Coefficient $C_p$ .....                                       | 44 |
| <b>Figure 18.</b> Contact Fatigue Strength for Through Hardened Steel Gears .....       | 44 |
| <b>Figure 19.</b> Parts of Press.....   | 47 |
| <b>Figure 20.</b> Stress-Strain Graphic .....   | 50 |
| <b>Figure 21.</b> Cross Section of Box of Gear .....                                    | 51 |
| <b>Figure 22.</b> Upper Die Technical Drawing .....                                     | 60 |
| <b>Figure 23.</b> Lower Die Technical Drawing.....                                      | 60 |
| <b>Figure 24.</b> Sheet Metal and Dies in ANSYS Discovery.....                          | 61 |
| <b>Figure 25.</b> U Bending Step 1 Analysis Settings .....                              | 62 |
| <b>Figure 26.</b> Copper Alloy Material Definitions .....                               | 63 |
| <b>Figure 27.</b> Contact Setting of Upper Die.....                                     | 64 |
| <b>Figure 28.</b> Contact Setting of Lower Die .....                                    | 64 |
| <b>Figure 29.</b> Meshed Sheet.....   | 65 |
| <b>Figure 30.</b> Patch Conforming Method Settings .....                                | 65 |
| <b>Figure 31.</b> Body Sizing Settings.....   | 66 |
| <b>Figure 32.</b> Face Sizing Settings .....  | 66 |
| <b>Figure 33.</b> Upper Die Displacement Settings .....                                 | 67 |
| <b>Figure 34.</b> Lower Die Displacement Settings.....                                  | 67 |
| <b>Figure 35.</b> Sheet Metal Displacement Settings.....                                | 67 |
| <b>Figure 36.</b> Maximum Press Moment in Step 1 .....                                  | 68 |
| <b>Figure 37.</b> The Moment When the Press First Stops in Step 1.....                  | 68 |
| <b>Figure 38.</b> Final State After Springback in Step 1.....                           | 69 |
| <b>Figure 39.</b> End of the First Step of U Bending.....                               | 69 |
| <b>Figure 40.</b> Part Transform Settings .....   | 70 |
| <b>Figure 41.</b> Contact Setting of Step 2 .....                                       | 71 |
| <b>Figure 42.</b> Maximum Press Moment in Step 2.....                                   | 71 |
| <b>Figure 43.</b> The Moment When the Press First Stops in Step 2.....                  | 71 |
| <b>Figure 44.</b> The Final State After Springback in Step 2 .....                      | 72 |
| <b>Figure 45.</b> Placement of the Sheet Metal into the Die for V-Bending .....         | 73 |
| <b>Figure 46.</b> Maximum Press Moment in V Bending .....                               | 74 |
| <b>Figure 47.</b> The Moment When the Press First Stops in V Bending .....              | 74 |
| <b>Figure 48.</b> Final State After Springback in V Bending .....                       | 75 |

## **LIST OF TABLES**

|   |    |
|---|----|
| <b>Table 1.</b> Properties of UNS C17200 Copper Alloy ..... | 32 |
| <b>Table 2.</b> Properties of AISI 4140 Steel.....          | 33 |
| <b>Table 3.</b> Overload Factor ( $K_o$ ).....              | 36 |
| <b>Table 4.</b> Empirical Constant A, B and C .....         | 39 |
| <b>Table 5.</b> End Condition Table.....                    | 52 |

## 1. INTRODUCTION

Metal forming methods encompass various processes such as forging, extrusion, rolling, and deep drawing. Among these, bending is a fundamental operation that uses plastic deformation to give sheet or plate parts a specific angle and geometry. Bending stands out for its practicality, low cost, and compatibility with a wide range of materials in both mass production and prototyping. [1]

The bending process works by driving the material from its elastic region into its plastic region—using machines or hand tools—so that it acquires a permanent angular shape. During this operation, tensile stresses develop on the outer surface of the workpiece while compressive stresses occur on the inner surface; once these stresses exceed the material’s yield strength, irreversible deformation takes place. As the metal bends, a neutral axis forms within the thickness to balance those stresses—but its position shifts depending on the material’s ductility and thickness. In thin sheets, the neutral axis generally lies near the geometric center, whereas in thicker plates it shifts inward. Therefore, selecting the optimal die radius based on sheet thickness and mechanical properties is critical in bending design. [2,3]

One of the most vital factors in successful bending is the compensation method. After the bending force is removed, the material releases some of its stored elastic energy, causing the bend to open up slightly—this is called “spring-back.” Spring-back can throw the final part angle out of tolerance, so operators often use an “over-bend” technique: bending the sheet a few degrees beyond the target angle to offset the expected rebound. In more sophisticated applications, work-hardening cycles or automatic CNC spring-back compensation values are calculated in advance and built into the bending program to ensure the correct final angle on every bend. [4]

Die design also plays a major role in bending quality. The die opening width, bend radius, and surface roughness all influence stress distribution and surface appearance. V-opening dies produce sharp, precise bends in thin sheets, while U-opening or custom-profile dies reduce cracking risk when forming larger radii. Smooth, well-lubricated die surfaces lower friction between the workpiece and die, extending die life and preventing scratches or distortions on the metal surface. [1]

Material type, thickness, and mechanical properties are the primary parameters in

bending. Steels, aluminum, and stainless steels each exhibit different yield behavior and spring-back amounts. For example, aluminum typically shows greater elastic deformation than steel, so it springs back more. As a result, spring-back compensation and die radius requirements for aluminum differ from those for steel. Increasing material hardness raises yield strength—which requires more bending force—but can also slightly reduce spring-back. [4]

Finally, planning a bending operation must account for bend sequence, bending speed, and workpiece clamping methods. When multiple bends are required, performing inward or nested bends first helps control overall deformation. Clamping the workpiece rigidly and bending with steady, vibration-free motion minimizes measurement errors and the need for rework. By harmonizing all these factors, manufacturers can achieve highly accurate, repeatable, and efficient bending operations for both one-off prototypes and mass-produced components. [1,3]

In the world of sheet-metal fabrication, a variety of techniques and processes—such as forging, extrusion, rolling, and deep drawing—are employed to turn metals into functional and aesthetic parts. Among these methods, the press brake process stands out for its precision, versatility, and widespread adoption.

A press brake is the central piece of equipment for industrial sheet-metal bending. Structurally, it consists of a fixed lower beam rigidly mounted in a frame and an upper beam (the ram) that moves vertically. A profiled lower die—typically V- or U-shaped—is seated on the lower beam, while the matching punch is mounted to the ram. When the ram is driven downward by hydraulic, mechanical, or electric actuation, the punch forces the workpiece into the die opening, plastically deforming it to the desired angle and bend radius. [5]

Achieving both efficiency and repeatability in press brake operations depends not only on punch and die geometry but also on the coordinated use of back-gauges, crowning systems, and spring-back compensation. A back-gauge positions the workpiece—either automatically or manually—to ensure each bend is made at the correct location and that final part lengths remain consistent. Crowning compensates for inevitable ram deflection by slightly raising the center of the lower beam relative to its ends, producing a uniform bend angle across the entire length of the sheet. In CNC machines, automatic spring-back

compensation routines analyze the material's elastic recovery and programmatically apply the precise "over-bend" required at each cycle.

Die-change speed and operator safety are also critical considerations. Quick-change tooling systems allow V-opening, U-opening, or custom-profile dies to be swapped in a matter of minutes, minimizing downtime. Light-curtain safety guards, two-hand control switches, and interlocking mechanisms protect operators, while intuitive CNC interfaces streamline setup and production workflows.

In small-scale workshops or mobile maintenance scenarios, large, stationary CNC press brakes prove too costly, unwieldy, and inflexible. For prototype production, urgent on-site repairs, and educational laboratories, there is a clear need for a low-tonnage, quickly deployable, easily portable bending tool that minimizes die-change downtime. Moreover, when working with thin sheet metals that do not require high tonnage, allowing the operator to feel the mechanics directly makes the process more intuitive and controlled.

Within this project, we have developed a "mini press brake" handheld device tailored to applications such as small-scale production environments, maintenance-repair shops, and teaching labs. The design goal was to achieve between 1 and 8 tons of static bending force purely through the operator's manual input—without any CNC systems, hydraulic pumps, or heavy steel frameworks—by means of a fully mechanical differential-gear-and-lever mechanism. As a result, the device offers:

- **Rapid setup:** Modular upper and lower dies (V-opening, U-opening, and custom profiles) can be changed in under 30 seconds using a quick-clamp system.
- **Portability:** The entire machine weighs no more than 12 kg and can be securely fixed to any work surface.
- **Easy maintenance:** The gear assembly's external housing provides straightforward access to lubrication and grease points.
- **Wide application range:** Capable of producing homogeneous bends in sheet thicknesses from 0.5 to 2 mm across various materials including alloy steels, stainless steels, and aluminum.

The developed mini press brake proves versatile in numerous contexts:

- **In-shop prototyping:** Rapid validation of design prototypes and model bending.

- **Field maintenance and repair:** Convenient mobile-unit integration for on-the-go equipment servicing.
- **Educational use:** Hands-on learning of bending principles for students.
- **Hobbyist and small-batch production:** A cost-effective, portable alternative for home workshops and SMEs.

In the following chapters, we will first present the theoretical foundations of the bending process and a literature review of press-brake designs; we will then detail our design criteria, mechanical calculations, manufacturing steps, and testing results. In doing so, we aim to deliver a low-cost, practical, and reliable manual bending solution tailored for small-scale production and educational use.

## 2. LITERATURE REVIEW

### 2.1. Bending

#### 2.1.1. Definition and Terminology

Bending is a most frequently encountered process in sheet metal forming. In some other forming processes, such as deep drawing, stretch flanging, bulging etc., bending is also involved although it is not a major feature. In the field of sheet metal bending, one can find literature on pure bending, V-die bending, simple flanging and so on. Most materials can be bent to quite a small radius. Failure may be a problem in bending of high-strength, less ductile sheets, but a greater problem is control of the shape of a bent workpiece. The bent workpiece will recover elastically i.e. springback on unloading and the bend quality is heavily dependent on the springback. The springback itself, however, is a function of material properties and process parameters such as Young's modulus, yield stress, strain hardening abilities, thickness and die geometry.

In fact, one of the most common processes for sheet metal forming is bending, which is used not only to form pieces such as L, U or V-profiles, but also to improve the stiffness of a piece by increasing its moment of inertia. Bending has the greatest number of applications in the automotive, aircraft and defense industries and for the production of other sheet metal products. Typical examples of sheet-metal bends are illustrated in Figure 1.

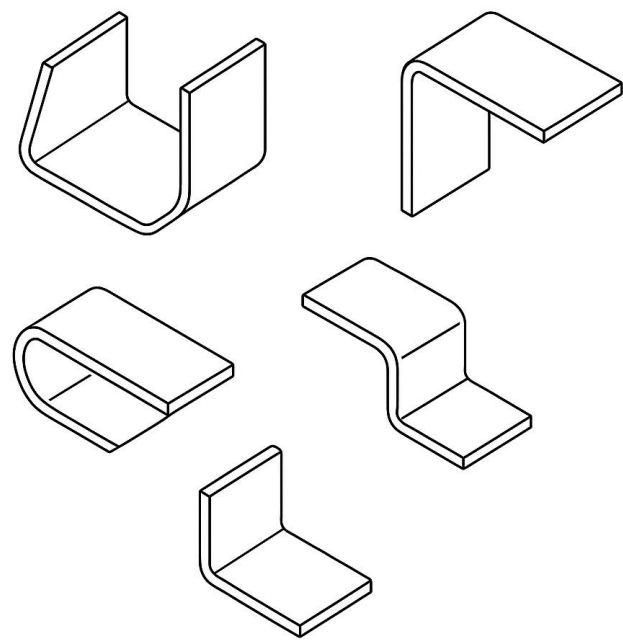


**Figure 1.** Typical examples of sheet metal bend parts.

In this sense, Neutral axis of a bended sheet defined in the drawing in Figure 2.

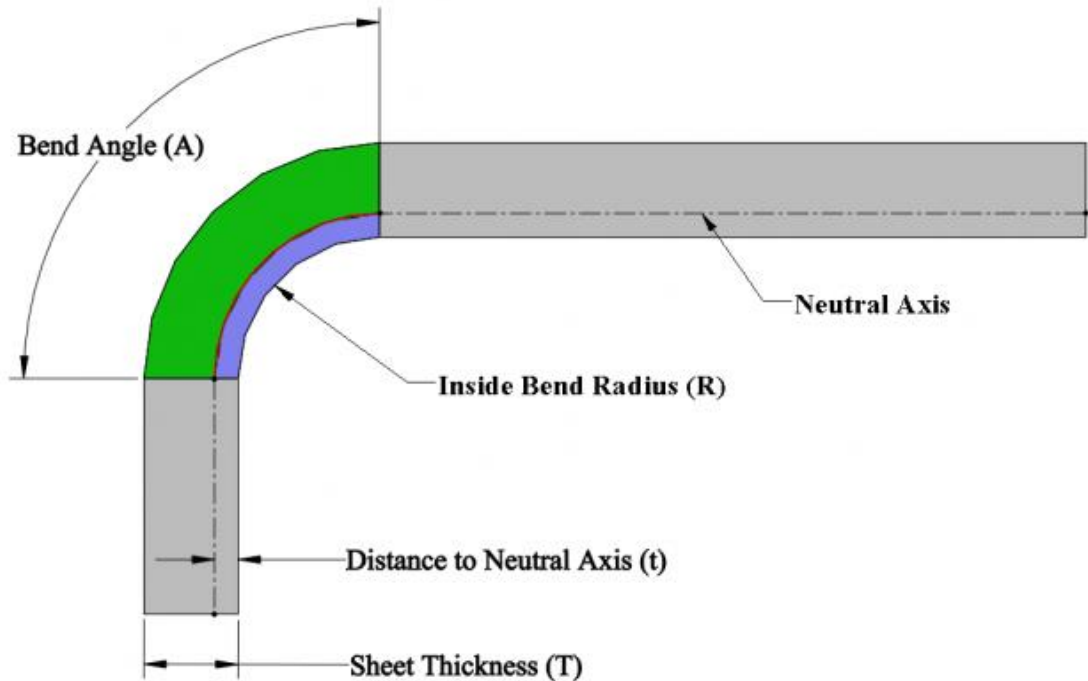


**Figure 2.** Neutral axis of a bended sheet

Here, the bend radius  $i R$  is measured on the inner surface of the bend piece. The bend

angle  $\phi$  is the angle of the bent piece and  $T$  is the material thickness.

During bending, the outermost fibers of the material are stretched while the innermost fibers are squeezed; in theory, the strains in these two regions have the same magnitude and can be expressed by the following formula:

$$e_0 = e_1 = \frac{1}{(2R_i/T)+1} \quad (2.1)$$

### 2.1.2. Moment of Bending

The bending moment is a fundamental concept in structural and mechanical engineering. It refers to the internal moment that resists the external loads applied to a structural element, such as a beam. When a load is applied perpendicular to the longitudinal axis of a beam, it creates internal stresses that tend to bend the beam. These internal stresses generate a rotational effect about a point or axis, which is defined as the bending moment.

[6]

Mathematically, the bending moment at a specific section of a beam is the sum of the moments due to external forces acting on one side of that section. It is expressed in units of force times distance (e.g., Newton-meters or N·m). The bending moment varies along the length of the beam depending on the type and distribution of loads, the beam's geometry, and its support conditions. [7]

In structural analysis, the bending moment is crucial for determining the stress distribution within the material, predicting deflections, and ensuring that the structure does not fail due to bending. Positive bending moments typically cause a beam to sag (concave upward), while negative bending moments cause it to hog (concave downward).

[8]

In design, engineers use bending moment diagrams to visualize and calculate the internal moments at different points along the structure, which then informs decisions on material selection, cross-sectional dimensions, and reinforcement requirements. [6]

In a deformable structural component subjected to gradually increasing external loads, yielding initiates once the stress state at a critical point first satisfies the yield criterion, commonly the von Mises or Tresca criterion depending on material properties. Upon further loading, plastic deformation begins to propagate, giving rise to a plastic zone

which expands into the surrounding elastic material. This plastic region is bounded by an elastic-plastic interface, the geometry of which is typically unknown and highly nonlinear. Consequently, the solution of such problems often necessitates the use of numerical methods, such as finite element analysis, to track the movement and shape of this boundary. [9]

When a component is designed based on the principles of elastic theory—such as simple bending or torsion—the allowable stress is determined by dividing the material's yield stress by a prescribed factor of safety. This ensures that under service loads, the maximum stress remains below the permissible level, thereby preventing permanent deformation. However, it is recognized that a component does not fail immediately upon reaching the yield point at localized regions, such as the outer fibers. Provided that a significant portion of the cross-section remains in the elastic range, the component retains its ability to carry further loads. To exploit this reserve strength, engineers may adopt a plastic limit design approach, which considers the formation of plastic hinges and redistributes internal moments until collapse. This method allows for a more efficient utilization of the material, especially in statically indeterminate structures. [9]

#### **2.1.2.1 Elasticity, Plasticity and Elastic-Plastic Domain**

**Elasticity** is a fundamental concept in the mechanics of solids that defines a material's ability to recover its original configuration after the removal of external loads. When the applied forces are small and do not exceed a specific threshold (the elastic limit), the deformation remains reversible. This behavior is mathematically described by Hooke's Law, which establishes a linear relationship between stress and strain. The constant of proportionality in this relationship is called the modulus of elasticity, which varies depending on the material's stiffness. The theory of elasticity enables engineers to predict how structures respond under service loads without experiencing permanent deformation. It is particularly critical in the initial design phase, where ensuring structural integrity within elastic limits is essential for safety and performance. [10]

**Plasticity**, in contrast, refers to the material's response once the stress exceeds the elastic limit. At this stage, the material undergoes irreversible deformation even after the external forces are removed. In the plastic region, the stress-strain relationship becomes nonlinear, and energy is dissipated within the material structure. This behavior is key in structural

applications where materials are subjected to high loads or intentional forming processes. Understanding plastic deformation is essential for defining the limits of material strength, especially in the context of failure prevention and forming analysis. [10]

**Elastic–plastic behavior** describes the transitional state where both elastic and plastic deformations coexist. When a body is subjected to gradually increasing loads, it initially responds elastically. Upon reaching the yield point, some regions begin to deform plastically, while others remain elastic. The body now contains distinct zones: an elastic domain governed by Hooke's Law, and a plastic domain experiencing permanent changes in geometry. This mixed behavior is particularly important in structural analysis, as it reflects real-world material response during service or forming operations. The boundary between these zones—often complex and dependent on geometry, loading, and material properties—requires numerical techniques for accurate analysis. [10]

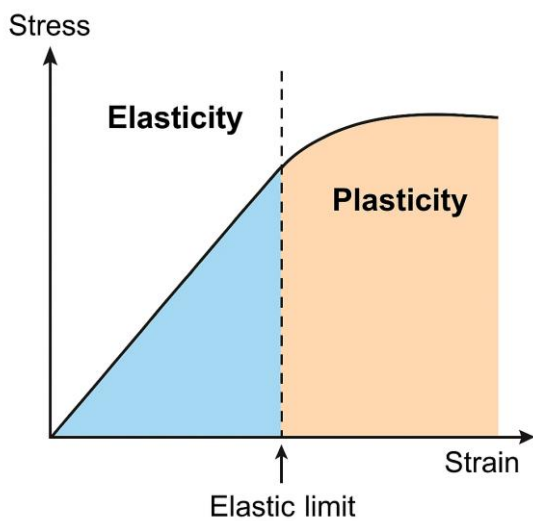


**Figure 3.** Elasticity, Plasticity and Elastic Limit

### 2.1.3. Types of Bending Operations

#### 2.1.3.1. V Bending

V-die bending is widely used throughout industry due to its simple tooling. During the V-die bending process, the punch moves downward, first coming into contact with the unsupported sheet metal. As it continues to move down, it forces the material to follow its motion until it bottoms out into the V-shape of the die at the final stage. [11]

In V-die bending, due to the mechanics of the process, the two end regions of the bent sheet lift off from the die and lean against the punch just before the fully loaded stage. As the punch continues to descend, the sheet ends are bent back toward the die, creating secondary bent-up regions on both sides, just above the main bent area. At the fully loaded state, the sheet is completely supported by both the die and the punch. [12] After removing the sheet from the punch and die, these secondary bent-up regions—which form during the bending process—also contribute to springback, occurring in the opposite direction of the springback caused by the main bent region. [11]

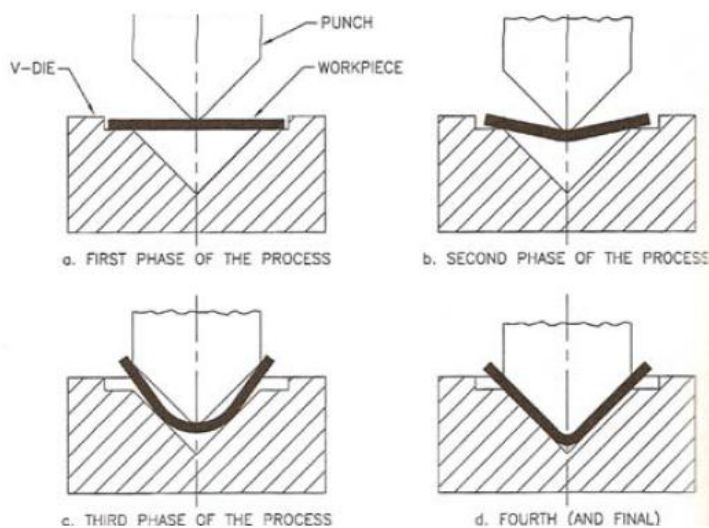


**Figure 4.** V-Die Bending

#### 2.1.3.2 U Bending

In this type of bending, the process starts by placing a strip or sheet of metal over a U-shaped opening or a die with such a shape. As the punch moves downward, it first makes contact with the sheet metal and pulls it along in its descent, then forces it into the U-shaped opening. [11]

In this case, to prevent the bottom from bulging outward during bending, a backing pad is commonly used. During the bending process, it begins to press against the bottom of the workpiece. [5]

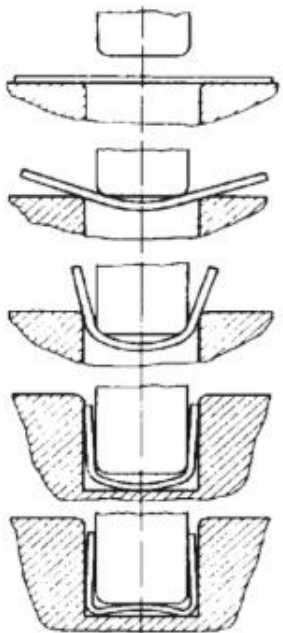


**Figure 5.** U-Die Bending

## 2.2. Springback

When producing a part, either by deep drawing, stretch forming or bending, flat sheet is transformed into a design shape and dimension. At the end of the forming process, when the part has been released from the forces of the forming tool, there is a distortion in the shape and dimension of the formed part. This distortion is termed springback. A depiction of springback in a simple bend can be seen in Figure 6. [1,5]

Springback is inherent in sheet metal forming. It can be understood by looking at a material's stress strain curve (discussed in the module on Tensile Testing) which characterizes the behavior of metal under applied force. During forming, the material is strained beyond the yield strength in order to induce permanent deformation. When the load is removed, the stress will return to zero along a path parallel to the slope of the elastic portion of the curve, which is the elastic modulus. This can be seen in Figure 7. The permanent deformation will therefore be less than what is designed into the part unless springback is factored in. [1,5]

Springback is dependent on various material characteristics but can be affected by tooling

design. The most important parameters are elastic modulus, strength, thickness, and bend radius. Other material characteristics, especially YPE, can also be important. [1,5]

Material with a higher elastic modulus will show less springback than material with a lower elastic modulus. This can be seen in Figure 7, where the unloading stress strain curve would be shifted toward less springback if it had a higher slope. However, between different types of steel there is essentially no difference in the elastic modulus so unless a totally different material is chosen, such as aluminum, this is not a consideration. [1,5]

A material with a higher yield strength will have a greater ratio of elastic to plastic strain and will exhibit more springback than material with a lower yield strength for a given amount of strain. [1,5]

Thickness is important because of how it impacts on strain. There is high total strain involved in bending a thick material around a given radius and low total strain involved in bending a thin material around the same radius. While under load, the total strain consists of both elastic and plastic strains. When the total strain is high, based on the stress strain curve, the relative amount of elastic strain is low. When the total strain is low, the relative amount of elastic strain is high and this results in more springback. It can be imagined that a very thin material could be bent around a radius with zero plastic strain. In this case the strain would be so low that it would be entirely elastic and the material would completely spring back to its original shape after the load is removed. Conversely a very thick material being bent over the same radius would show a very high total strain. The absolute value of the elastic portion of the strain would be similar to that of the thin material but it would be insignificant compared to the plastic portion of the strain. Therefore, the thick material would show very little springback. [1,5]

Another material characteristic worth mentioning is the Yield Point Elongation (YPE). YPE is the strain associated with discontinuous yielding that can occur when steel is placed in tension. It is well demonstrated that steel showing a pronounced YPE shows less springback than steel with no YPE. In the case of steel with a high YPE more of the stress is used to concentrate thinning locally resulting in a lower proportion of total strain that is elastic and hence less springback. One would think that this parameter can be used to effectively reduce springback. However, that is not always the case because YPE is variable, between coils, within coils, and is directional, so its effects can be variable. In

general variability can be more problematic than the absolute value of springback. [1,5]

Methods of addressing springback include process design and part design. In terms of the process, overbending, retarding metal flow due by use of draw beads and higher binder pressure, using lower press speeds, restriking, applying tension during bending, using tighter die clearances, are all techniques that are used. In terms of part design, by utilizing tooling configurations that force higher strain over a small area springback can be minimized. [1,5]

As well there are angle compensation feedback mechanisms that are able to make automatic adjustments for each piece. [1,5]

Finally, there are modeling techniques that attempt to analyze three dimensional parts so that the tooling can be designed to compensate for springback. [1,5]

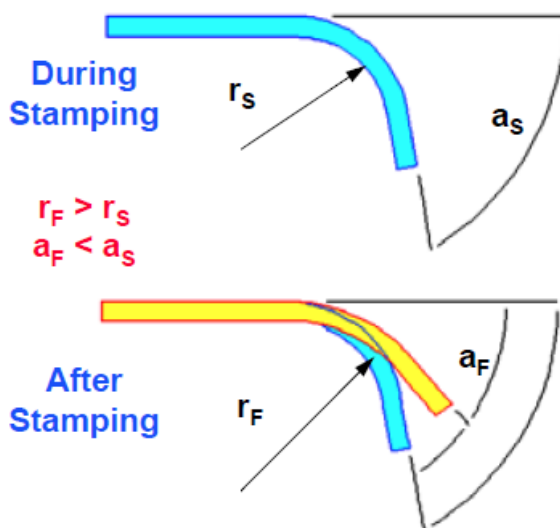


**Figure 6.** Elastic Springback

(r=radius, a = angle, s = start, f = finish)

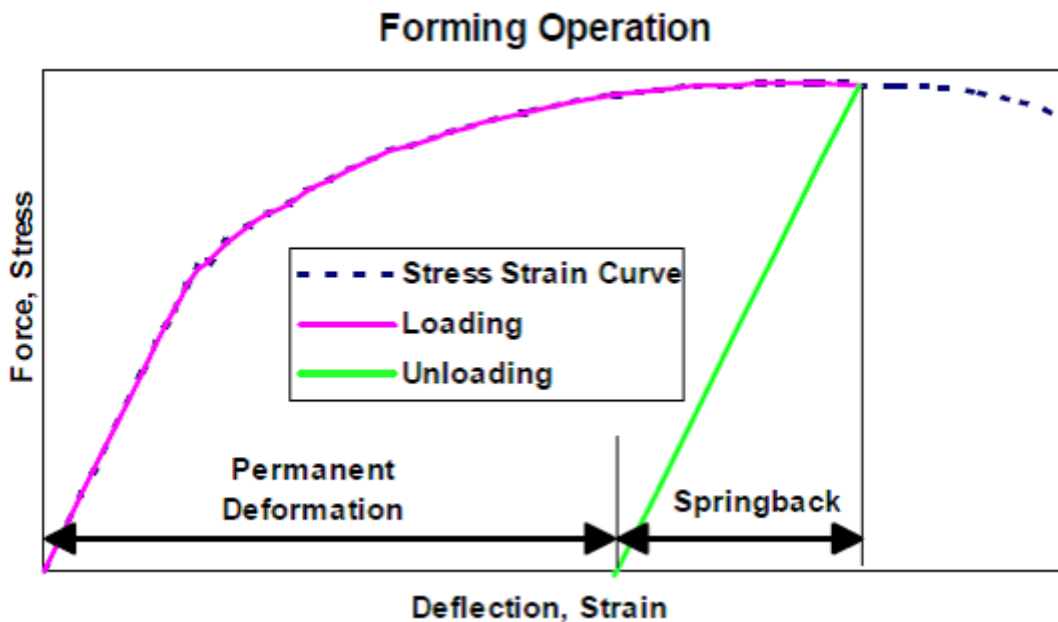


**Figure 7.** Strain and Stress Behaviour During the Forming Process

### 2.3. Advantages and Disadvantages of Bending Process

The bending process is one of the most widely used methods in metal forming due to its simplicity, efficiency, and suitability for mass production. As described by Kalpakjian and Schmid, one of the primary advantages of bending is its ability to transform flat sheet metal into complex shapes without the need for material removal. Since it is a chipless forming method, material waste is minimal, leading to high material efficiency. This is particularly beneficial in industries where cost control and material conservation are critical. [1]

Another significant advantage is the adaptability of the bending process to various production volumes. It is highly compatible with automated systems and can be easily integrated into production lines, allowing high-speed manufacturing with consistent quality. The process is also capable of producing a wide range of geometries such as V-bends, U-bends, channels, flanges, and hems, making it versatile for applications in automotive, aerospace, and appliance industries. [13]

From a mechanical perspective, bending can improve certain properties of the material. During plastic deformation, the metal undergoes strain hardening, which can increase its strength and hardness in the bent region. This can be desirable in components that require localized strengthening. Furthermore, because bending is often performed as a cold working process, the surface finish of the material is preserved, and tight dimensional

tolerances can be achieved without secondary machining operations. [2]

However, despite these advantages, the bending process also presents several limitations. One major disadvantage is the high initial cost associated with tooling. Precision dies, punches, and hydraulic or mechanical presses are necessary for accurate and repeatable results, and these components can be expensive to design, manufacture, and maintain. For custom or low-volume production, the cost of tooling may not be justified.

Material limitations also play a role in defining the boundaries of the bending process. Not all metals respond favorably to bending; brittle or low-ductility materials are prone to cracking or fracturing under tensile stress, especially on the outer radius of the bend. In such cases, additional heat treatments or process modifications may be required to reduce the risk of failure.

Tool wear is another challenge in the bending process. Over time, the constant application of force and friction between the tools and workpieces leads to wear on the die and punch surfaces. This necessitates regular maintenance or replacement, which can increase downtime and operational costs. Additionally, the bending process requires significant control and precision, particularly when forming thin sheets, where issues such as springback and distortion are common. Springback, which refers to the elastic recovery of the material after the bending force is removed, can lead to deviations from the desired angle and shape, requiring compensation through overbending or tooling adjustments.

Thickness and bend radius also influence the behavior of the material during bending. Thinner materials tend to show greater springback due to a higher proportion of elastic strain relative to plastic strain. Conversely, thicker materials, while easier to form with less springback, require higher forming forces and more robust equipment.

Lastly, while springback can be mitigated through process and tool design—such as by applying tighter die clearances, restriking the part, or introducing draw beads—it cannot be entirely eliminated. Variability in material properties, such as yield point elongation (YPE), further complicates prediction and control, especially when using steels with inconsistent YPE behavior across different coils or orientations. [1]

In summary, while bending remains a fundamental and efficient forming method in modern manufacturing, it is not without its technical and economic challenges. A thorough understanding of material behavior, process parameters, and tooling design is

essential for optimizing performance and minimizing defects. As Groover suggests, successful application of bending depends on balancing its many benefits—such as speed, cost-efficiency, and versatility—against its inherent limitations, including tooling costs, material constraints, and control requirements.

#### 2.4. Press Brake Process

The press brake process is a widely adopted sheet metal forming method used to produce angular bends in metal workpieces with high accuracy and repeatability. This process involves clamping a flat sheet or plate between a punch and die, and applying force through a press brake machine to plastically deform the material into a desired angle or profile. The deformation primarily occurs along a linear axis, making the process suitable for a wide variety of geometries, including V-bends, U-bends, channels, flanges, and hems. [2]

At its core, press brake bending relies on plastic deformation. When the punch descends and presses the sheet into the die, the material initially undergoes elastic deformation and then yields plastically once the stress exceeds the yield point. Upon release of the punch, springback occurs due to the recovery of the elastic strain. This phenomenon must be compensated for during the process, often by slightly overbending the sheet to ensure dimensional accuracy in the final part. [2]

Press brake systems can be classified as manual, hydraulic, mechanical, or servo-electric, with CNC press brakes being the industry standard for high-precision and repeatable manufacturing. CNC control allows for programmable back gauges, automatic angle corrections, and real-time monitoring of force and position, making modern press brakes highly efficient and flexible. [1]

The process is characterized by several key parameters:

- Material properties: including yield strength, elastic modulus, and thickness
- Punch and die geometry: such as punch radius and die opening width
- Bending length and angle
- Bend allowance and deduction
- Press tonnage requirements

Applications of the press brake process span across multiple industries such as automotive, aerospace, construction, furniture, and electrical enclosures, due to its adaptability to complex geometries and low tooling costs compared to stamping or deep drawing. It is especially valuable in low-to-medium volume production where setup flexibility is essential [14].

Despite its advantages, the process has some limitations. These include:

- Sensitivity to springback, especially in high-strength materials like aluminum alloys
- Dependence on tooling accuracy and alignment
- Limitations in forming very tight radii without cracking, especially in brittle materials

With recent advancements, finite element analysis (FEA) and simulation software have allowed engineers to predict deformation behavior, springback, and required forces with high precision, significantly reducing trial-and-error in tooling setup [5].

#### **2.4.1. Origin and Industrial Significance of The Press Brake Process**

Press brake technology has evolved as a fundamental solution in modern sheet metal manufacturing, particularly addressing the need for precision, repeatability, and cost-efficiency in bending operations. Initially, it emerged in response to significant structural and operational inefficiencies in traditional bending techniques, which were unable to meet the growing demand for flexible and adaptive manufacturing systems.

##### **2.4.1.1. Limitations of Traditional Bending Methods**

Conventional sheet metal bending methods typically relied on fixed dies, limiting production to specific product geometries and requiring frequent and time-consuming tool changes. This rigid structure posed challenges in dynamic industrial environments where rapid prototyping and customized designs are critical.

##### **2.4.1.2. Inconsistencies in Precision and Quality**

Due to reliance on manual processes, conventional systems often resulted in dimensional inconsistencies, leading to quality degradation and increased rejection rates. CNC-

enabled press brakes offer superior control and repeatability, significantly improving production accuracy.

#### **2.4.1.3. Efficiency and Process Management Issues**

Traditional setups also suffered from low process efficiency, particularly during product changeovers. The introduction of programmable press brakes has streamlined workflow continuity by reducing setup times and enabling faster transitions between production cycles.

#### **2.4.1.4. Inability to Adapt to Variable Designs**

The ability to integrate press brakes with CAD/CAM software provides enhanced design flexibility, allowing seamless transfer of digital models to physical components. This capability is especially advantageous in short-run or high-mix manufacturing environments.

#### **2.4.1.5. Search for Cost Advantage**

Tooling costs have historically been a barrier to cost-effective small-batch production. Press brakes mitigate this challenge through the use of universal dies and flexible configurations, reducing tooling expenses significantly.

#### **2.4.1.6. Contribution of Press Brake Technology to Industry**

Press brake technology has evolved as a fundamental solution in modern sheet metal manufacturing, particularly addressing the need for precision, repeatability, and cost-efficiency in bending operations. Initially, it emerged in response to significant structural and operational inefficiencies in traditional bending techniques, which were unable to meet the growing demand for flexible and adaptive manufacturing systems.

### **3. HANDMADE PRESS BRAKE MACHINE SETUP**

In this project, a manually operated mini press brake—fully constructed in a workshop environment—was used to perform precise bending operations on thin copper sheets. The system is based on a rack and pinion mechanism, allowing the downward motion of the upper punch to be controlled by a hand-operated lever. Thanks to its simplicity and portability, the system proves highly efficient for small-scale production, prototyping,

and forming of custom geometries.

The fixed lower die and movable upper punch (both visible in the assembly) are designed to produce near-90° bends. The red vertical track shows the rack, which engages with the pinion gear to convert rotational input into linear motion. The upper punch thus travels downward smoothly and steadily. The die block and baseplate are made with sufficient rigidity and are securely welded, minimizing springback and ensuring stable results during bending.

The process starts with positioning the copper alloy sheet (99% Cu) or pure copper on the V- or U-shaped lower die. By rotating the handle clockwise, the user lowers the upper punch, applying controlled force to bend the sheet at the desired angle. As shown in the second image, the result is a clean, sharp-edged workpiece. Depending on the material's thickness and springback characteristics, an overbending technique may be applied to ensure dimensional accuracy after unloading.

While this manual press brake produces lower force compared to hydraulic systems, it is sufficient for thin and ductile metals like copper, aluminum, and brass. It also provides excellent precision by enabling direct operator control. In conclusion, this low-cost, small-scale, human-powered solution successfully demonstrates the feasibility and effectiveness of manual forming techniques in engineering applications.

### **3.1. Parts of Hand Made Press Brake**

#### **3.1.1. Upper Die (Punch)**

The upper die, commonly referred to as the punch, is a core element of any press brake system. It is responsible for delivering the forming force required to bend the sheet metal against a lower die. Typically manufactured from hardened tool steel or alloy steel, punches are designed with specific profiles to achieve various bend angles and radii. Their geometry determines the precision and quality of the final workpiece. Standard punches include acute, gooseneck, radius, and hemming punches, each serving different applications. Accurate alignment and uniform pressure distribution are critical features of an effective punch, ensuring minimal material distortion and consistent part dimensions.

In our mini press brake project, the upper die is a solid red-painted steel structure housed within the vertically moving unit. It has been custom-shaped to interface with the fixed

die below and produce bends at a controlled angle. The punch is mounted onto the rack system and is actuated manually through a rack and pinion mechanism. Its robust construction and firm alignment are essential to producing clean, uniform bends without relying on hydraulic or pneumatic pressure.

### **3.1.2. Lower Die (Base Die Block)**

The lower die is the stationary tool in a press brake setup that works in conjunction with the punch to deform the sheet metal. This die typically features a V-shaped or U-shaped groove, into which the material is pressed. The size of the groove and the angle formed within it dictate the resulting bend angle and radius. Lower dies are often changeable to accommodate various material thicknesses and desired bends. Made of tool steel, they must resist significant compressive stress and maintain dimensional stability over time.

In our project, the lower die is fixed directly onto the baseplate of the machine and machined to provide a sharp, controlled reaction surface. Its position ensures that the punch aligns precisely with it during operation. Due to the absence of automated controls, the die's accurate placement and robust mounting are vital in maintaining consistent bending geometry throughout the operation.

### **3.1.3 Rack and Pinion Mechanism**

The rack and pinion mechanism is a classic mechanical system that converts rotational motion into linear displacement. It comprises a circular gear (the pinion) engaging with a linear toothed component (the rack). This mechanism is widely used in automotive steering systems, manual elevators, and machinery requiring controlled linear actuation. It offers mechanical advantage, enabling the application of large linear forces with minimal rotational input. Key features include low maintenance, compact design, and high reliability in force transmission.

In our mini press brake, the rack is fixed vertically and integrated into the housing that holds the punch. The operator rotates the handle attached to the pinion, which in turn drives the rack downward, moving the punch into the die. This setup allows for fine manual control, enabling small adjustments and repeatable press actions without external power. The accuracy and simplicity of this mechanism play a central role in the overall usability of the device.

### **3.1.4. Manual Handle (Crank Arm)**

The manual handle, or crank arm, is a lever tool used to apply torque to a mechanical system. In general mechanical design, crank arms are utilized to impart rotational force with improved

mechanical leverage. They are found in a variety of tools and machines, ranging from old-fashioned drills to modern manual mills. Ergonomic knobs, length, and angular positioning of the handle are key to operator comfort and control.

For our device, the manual handle is directly connected to the pinion gear of the rack and pinion assembly. The handle's design allows the user to apply substantial torque with minimal effort, enabling precise punch movement even during thicker metal bending. Its positioning also ensures that the user's force is consistently and safely transmitted, contributing to smooth and predictable operation.

### **3.1.5. Support Column and Machine Base**

In machinery, the support column serves as the guiding and stabilizing structure that ensures axial movement and alignment. Support columns are essential in drill presses, milling machines, and other vertical tools. They are typically made of solid or thick-walled tubing and are fixed to a baseplate, which provides structural anchorage and distributes mechanical loads to the floor or a workbench. Together, these parts form the machine's skeleton.

In our mini press brake, the cylindrical support column ensures that the vertical motion of the punch remains straight and linear. It prevents lateral displacement and ensures that the rack engages the pinion evenly throughout the stroke. The baseplate, made from thick steel, anchors the entire unit, providing a stable work surface that absorbs vibrations and force impacts. This structural assembly ensures durability, repeatability, and user safety, particularly in the absence of electronic control systems.

### **3.1.6 Adjustable Back Gauge**

adjustable back gauge mechanism used for positioning the sheet metal before the bending operation. This back gauge allows the operator to align the sheet piece at the same reference point each time, ensuring repeatability and dimensional accuracy for every bend. The mechanism features a manually adjustable rail or guide system and can be moved forward or backward to accommodate different part lengths. This ensures consistent measurements during mass production while also saving time. Additionally, by enabling the operator to predefine the bending length, the risk of incorrect placement is minimized. Such back gauge systems offer significant advantages, especially in small and portable press brake devices, as they allow for rapid transitions between different sheet sizes without the need to change tooling.



**Figure 8.** Mini Press Brake

### 3.2. Materials

#### 3.2.1 UNS C17200 Copper Alloy

In our project, a copper alloy was used as the material for experimental bending applications due to its excellent ductility, high thermal conductivity, and sufficient strength properties. The selected copper alloy resembles the characteristics of UNS C17200 (Beryllium Copper), widely known for its high copper content (approximately 98%). This alloy is often used in bending and forming.

The mechanical properties such as tensile yield strength of 280 MPa, along with a Young's modulus of  $1.10 \times 10^5$  MPa, suggest that this material can endure moderate mechanical stress while still allowing precise plastic deformation with minimal springback. With a Poisson's ratio of 0.34 and bulk modulus of  $1.145 \times 10^5$  MPa, the alloy also demonstrates stable volumetric elasticity. The density of the material is  $8.3 \times 10^{-6}$  kg/mm<sup>3</sup>, confirming the lightweight yet robust nature of the alloy.

These properties make it suitable for processes press-brake bending. Its consistent plastic deformation characteristics provide a reliable base material for manufacturing precision components without significant dimensional loss due to springback.

**Table 1.** Properties of UNS C17200 Copper Alloy

| Property                  | Value                | Unit               |
|---------------------------|----------------------|--------------------|
| Elastic Modulus           | 150                  | GPa                |
| Density                   | $8.3 \times 10^{-6}$ | kg/mm <sup>3</sup> |
| Young's Modulus           | $1.10 \times 10^5$   | MPa                |
| Poisson's Ratio           | 0.34                 | —                  |
| Bulk Modulus              | $1.145 \times 10^5$  | MPa                |
| Shear Modulus             | 41,045               | MPa                |
| Yield Strength            | 280                  | MPa                |
| Ultimate Tensile Strength | 430                  | MPa                |

### 3.2.2 AISI 4140 Steel

AISI 4140 is a versatile low-alloy steel that contains chromium, molybdenum, and manganese as its primary alloying elements. It belongs to the family of medium carbon steels and is widely known for its exceptional strength, toughness, and fatigue resistance. These properties make it an ideal candidate for components that must withstand high mechanical loads and demanding service conditions, such as gears, shafts, spindles, bolts, crankshafts, and structural parts used in the aerospace, automotive, and oil & gas industries.

One of the key advantages of AISI 4140 is its excellent balance between hardness and ductility. When heat treated (typically quenched and tempered), this alloy achieves a ultimate tensile strength of up to 655 MPa and a yield strength around 415 MPa, while maintaining elongation and toughness necessary to avoid brittle failure. The alloy can also be nitrided to further increase surface hardness and wear resistance without compromising core toughness, making it highly suitable for sliding and rotating parts subjected to surface stresses.

In addition to its mechanical robustness, AISI 4140 is also used in design applications where dimensional accuracy, repeatable mechanical response, and surface finish quality are essential. Due to its alloying content, it is more resistant to deformation and fatigue cracking than plain carbon steels.

AISI 4140 conforms to standards such as ASTM A29, SAE J404, and UNS G41400. Depending on the delivery condition—annealed, normalized, or quenched and tempered—its properties can be tailored for both static and dynamic loading environments. This flexibility makes AISI 4140 one of the most preferred materials in the

engineering world where performance and reliability must go hand in hand.

**Table 2.** Properties of AISI 4140 Steel

| Property                  | Value                 | Unit               |
|---------------------------|-----------------------|--------------------|
| Elastic Modulus           | 210                   | GPa                |
| Density                   | $7.85 \times 10^{-6}$ | kg/mm <sup>3</sup> |
| Poisson's Ratio           | 0.30                  | —                  |
| Bulk Modulus              | 140                   | GPa                |
| Shear Modulus             | 80                    | GPa                |
| Yield Strength            | 415                   | MPa                |
| Ultimate Tensile Strength | 655                   | MPa                |
| Hardness, Brinell         | 197                   | -                  |
| Reliability               | 0.99                  | -                  |

### 3.4. Calculations

#### 3.4.1. Gear

**Gear Bending Stress Equation:** It is the stress caused by the bending effect of the force applied to the gear in the tooth root area. This stress occurs especially with the load on the tooth tips while the gear is rotating and can cause the tooth to break or fatigue over time. It is one of the most critical types of stress in terms of gear durability and is affected by factors such as tooth shape, material, module, and load direction. Therefore, it must be carefully calculated in the design. [15]

$$\sigma = W^t K_O K_V K_S \frac{K_H K_B}{bm_t Y_J}$$

**Bending Factor of Safety:** It is a ratio that shows the safety of the gear against bending stress. It is the ratio of the maximum bending stress that the gear can withstand to the actual bending stress acting on it. This coefficient is used to reduce the risk of gear breakage or damage and is determined in order to provide adequate safety in the design. [15]

$$S_F = \frac{S_t Y_N}{Y_\theta Y_Z \sigma}$$

**Gear Contact Stress Equation:** It is the compressive stress that occurs on the contact surfaces of gears, especially in the area where the tooth surfaces come into contact with each other. This stress can cause damage such as wear, crushing or cracking on the

tooth surfaces. It is a very important parameter in terms of the life and performance of gears and is calculated depending on the durability of the contact surface, material properties and load distribution. [15]

$$\sigma_C = Z_E \sqrt{W^t K_O K_V K_S \frac{K_H Z_R}{d_{w_1} b Z_1}}$$

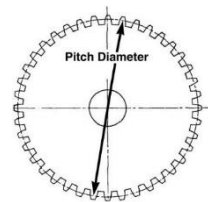
**Wear Factor of Safety:** It is a ratio that shows the level of safety provided against wear on the contact surface of gears. In order for the tooth surfaces to operate for a long time without being damaged due to wear, it is evaluated as the ratio of the expected wear amount to the wear limit that the tooth material can withstand. This coefficient is taken into account in the design to extend the life of the gear and prevent failures. [15]

$$S_H = \frac{S_C Z_N Z_W}{Y_\theta Y_Z \sigma_C}$$

**Transmitted Load (W<sup>t</sup>):** This is the actual contact force on the tooth surface, and this force is a fundamental value in both the strength calculations of the gear material and in wear and strength analyses. [16]

$$W^t = \frac{60000H}{\pi dN}$$

#### Pitch Diameter ( $d_p$ )



**Speed (N):** There is no clear measurement for gear speed. In this mechanism, since the

**Figure 9.** Pitch Diameter of Gear

gear is rotated by a human, a speed that can be rotated by human power is assumed.

$$N = 90 \text{ rev/min}$$

**Horsepower (H):** It is a unit of measurement that expresses the work done or the power produced per unit time. [17]

$$H = \frac{2\pi NT}{60}$$

**Torque (T):** It is the force effect that initiates and maintains the rotational motion of an object. In other words, it is the rotational force around an axis. [15]

$$T = F \cdot r$$

**Force (F):** Since the force is applied by a human, a net force value cannot be used. For this reason, the force value that a human can produce is assumed.

$$F = 150 \text{ N}$$

**Length of arm:** 0.2 m.

$$T = 150 \cdot 0.2 = 30 \text{ Nm}$$

$$H = \frac{2\pi \cdot 90 \cdot 30}{60} = 282.74 \text{ W}$$

$$W^t = \frac{60000 \cdot 282.74}{\pi \cdot 45 \cdot 90} = 1333.32 \text{ N}$$

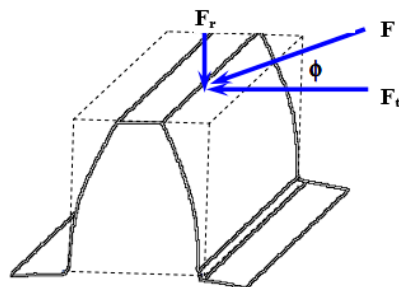


**Figure 10.** Forces on the Tooth of Gear

**Pressure Angle ( $\phi$ ):** It is the angle between the direction of the force at the tooth contact point and the line drawn perpendicular to the pitch circle of the gear to which this point is tangent. [18]

$$\phi = 20^\circ$$

**Tangential Force ( $F_t$ ):** Tangential component of the force in contact with the tooth surface in gears, tangential to the direction of rotation of the gear. This force causes the gear to rotate the other gear and plays a direct role in the generation of torque. This force in gears equal to transmitted load. [18]

$$F_t = W^t = 1333.32 \text{ N}$$

**Radial Force ( $F_r$ ):** It is the component of the tooth contact force in gears that is directed towards the center of the gear. It does not contribute to the rotational motion but represents the force on the gear shaft or bearing. [18]

$$F_r = F_t \cdot \tan 20 = 1333.32 \cdot \tan 20 = 485.29 \text{ N}$$

**Overload Factor ( $K_o$ ):** It represents the effect of unexpected overloads such as sudden impacts, load changes or usage errors that may occur during gear operation. [19]

### DRIVEN MACHINE

**Table 3.** Overload Factor ( $K_o$ )

| POWER SOURCE        | UNIFORM | MODERATE SHOCK | HEAVY SHOCK |
|---------------------|---------|----------------|-------------|
| <b>UNIFORM</b>      | 1       | 1.25           | 1.75        |
| <b>LIGHT SHOCK</b>  | 1.25    | 1.5            | 2           |
| <b>MEDIUM SHOCK</b> | 1.5     | 1.75           | 2.25        |

The bending process is done in the arbor press machine. This machine presses the desired sheet metal and applies shear on the sheet metal. Therefore, driven machine, heavy shock is selected. Since this machine works with human power, the power source is determined as uniform.

$$K_o = 1.75$$

**Dynamic Factor ( $K_v$ ):** It is a coefficient that takes into account the dynamic effects caused by vibration and speed to which gears are subjected while operating. The lower the speed and quality, the lower the  $K_v$ ; as speed and defect increase, the higher the  $K_v$ . [15]

$$K_V = \left( \frac{A + \sqrt{200V}}{A} \right)^B$$

$$A = 50 + 56(1 - B)$$

$$B = 0.25(12 - Q_V)^{2/3}$$

**Pitch Line Velocity (V):** It is the linear velocity of points on the pitch circle of a gear. [15]

$$V = \frac{\pi dN}{60} = \frac{\pi \cdot 0.045 \cdot 90}{60} = 0.212 \text{ m/s}$$

**Quality Value Ranges (Qv):** It is a measure of quality criteria such as gear surface smoothness, tooth error, manufacturing tolerances and assembly accuracy, and the larger the number, the higher the quality. [15]

- 3-6: Low sensitivity (agricultural machinery)
- 7-8: Medium sensitivity (automotive transmission)
- 9-12: High sensitivity (machine tool)

The Qv value is obtained from the manufacturer and the value in this project is 10.

$$B = 0.25(12 - 10)^{2/3} = 0.39685$$

$$A = 50 + 56(1 - 0.39685) = 83.77639$$

$$K_V = \left( \frac{83.77639 + \sqrt{200 \cdot 0.212}}{83.77639} \right)^{0.39685} = 1.03$$

**Size Factor (Ks):** It represents the stress distribution and defect effects in the material that occur depending on the size of the gear. The effect of material defects can be more pronounced in large gears, so it is necessary to increase the stress for safety. In small gears, this value is taken as 1. [15]

$$K_S = 1$$

**Load Factor ( $K_H$ ):** It is used to take into account the load changes, fluctuations and impacts that occur depending on the environment and load conditions in which the gear operates. [15]

$$K_H = 1 + C_{mc}(C_{pf}C_{pm} + C_{ma}C_e)$$

**Load Correction Factor ( $C_{mc}$ ):** It is a correction factor used to account for factors such as fluctuations in the actual operating conditions of the load to which the gear is exposed, sudden load increases or differences in load distribution. [15]

$$C_{mc} = \begin{cases} 1 & \text{for uncrowned teeth} \\ 0.8 & \text{for crowned teeth} \end{cases}$$

$$C_{mc} = 1 \text{ for this pinion}$$

**Pinion Proportion Factor ( $C_{pf}$ ):** It is a coefficient used in gear design and is used to correct the effect of the load on the pinion depending on the size and load ratios of the gear mating with the pinion. [15]

$$C_{pf} = \begin{cases} \frac{F}{10d_p} - 0.025 & F \leq 1 \text{ in} \\ \frac{F}{10d_p} - 0.0375 + 0.0125F & 1 < F \leq 17 \text{ in} \\ \frac{F}{10d_p} - 0.1109 + 0.0207F - 0.000228F^2 & 17 < F \leq 40 \text{ in} \end{cases}$$

## Face Width (F)

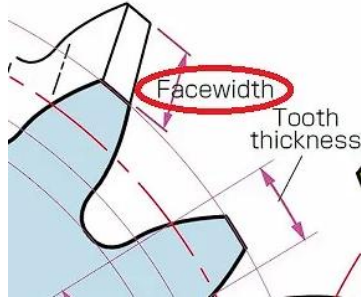


**Figure 11.** Face Width of Gear (F)

$$F = 25 \text{ mm} = 0.984 \text{ inch}$$

The first interval is taken because it is less than 1 inch.

$$C_{pf} = \frac{0.984}{10 \cdot 1.772} - 0.025 = 0.0305$$

**Pinion Proportion Modifier (C<sub>pm</sub>):** It means the proportional modification made depending on the geometrical features of the pinion when calculating the strength and load carrying capacity of the pinion. [15]

Since there is no bearing in the mechanism, this value is taken as 1 directly.

**Mesh Alignment Factor (C<sub>ma</sub>):** It is a factor that shows how accurately and properly aligned the points where the gears come into contact with each other are. If the gears are not fully aligned, the contact surface decreases and the load carrying capacity decreases. [15]

$$C_{ma} = A + BF + CF^2$$

**Table 4.** Empirical Constant A, B and C

| CONDITION      | A      | B      | C                         |
|----------------|--------|--------|---------------------------|
| OPEN GEARING   | 0.247  | 0.0167 | -0.765(10 <sup>-4</sup> ) |
| COMMERCIAL     | 0.127  | 0.0158 | -0.930(10 <sup>-4</sup> ) |
| PRECISION      | 0.0675 | 0.0128 | -0.926(10 <sup>-4</sup> ) |
| EXTRAPRECISION | 0.0036 | 0.0102 | -0.822(10 <sup>-4</sup> ) |

In this mechanism, it falls into the commercial class.

$$C_{ma} = 0.127 + 0.0158 \cdot 0.98425 - 0.930(10^{-4}) \cdot 0.98425^2 = 0.14246$$

**Mesh Alignment Correction Factor (C<sub>e</sub>):** It is a correction factor used in gear design and accounts for deviations in the alignment of the mesh between gears. [15]

$$C_e = \begin{cases} 0.8 & \text{for gearing adjusted at assembly, or compatibility is improved by lapping} \\ 1 & \text{for all other conditions} \end{cases}$$

$$C_e = 1 \text{ for this pinion}$$

$$K_H = 1 + 1(0.0305 \cdot 1 + 0.14246 \cdot 1) = 1.17$$

**Rim Thickness Factor (K<sub>B</sub>):** It is a factor that measures the resistance of the teeth against breakage or deformation, depending on the thickness of the back surface (rim) on which the gear teeth rest. A thin or weak rim negatively affects the strength of the teeth. [15]

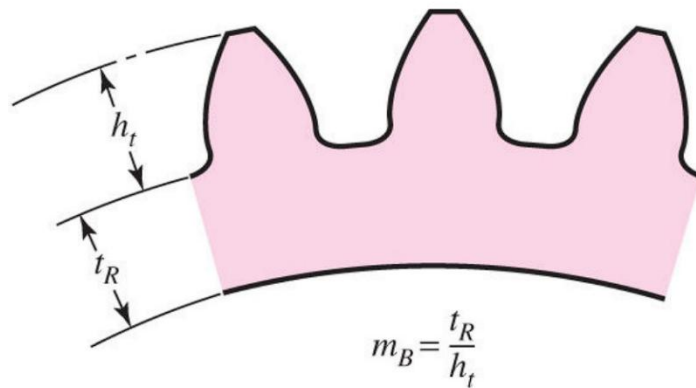


**Figure 12.** Rim Thickness and Tooth Height of Gear

$$K_B = \begin{cases} 1.6 \ln \frac{2.242}{m_B}, & m_B < 1.2 \\ 1, & m_B \geq 1.2 \end{cases}$$

- Rim thickness ( $t_r$ ): 9.75 mm
- Tooth height ( $h_t$ ): 5.5 mm
- Back-up ratio ( $m_B$ )

$$m_B = \frac{9.75}{5.5} = 1.77$$

$$K_B = 1 \text{ for this pinion}$$

**Half Width (b):** It shows the contact length of the 2 cylinders. In gear mechanisms, this length is taken as facewidth. [15]

$$b = F = 25 \text{ mm}$$

**Transverse Module ( $m_t$ ):** It equal to module on spur pinion. [15]

$$m_t = m = 2.5 \text{ mm}$$

**Bending Strength Geometry Factor ( $Y_J$ ):** It is the geometry factor that determines the bending strength of the gear. It affects the bending stress depending on the tooth profile and shape and is taken into account to reduce the risk of gear breakage. [15]

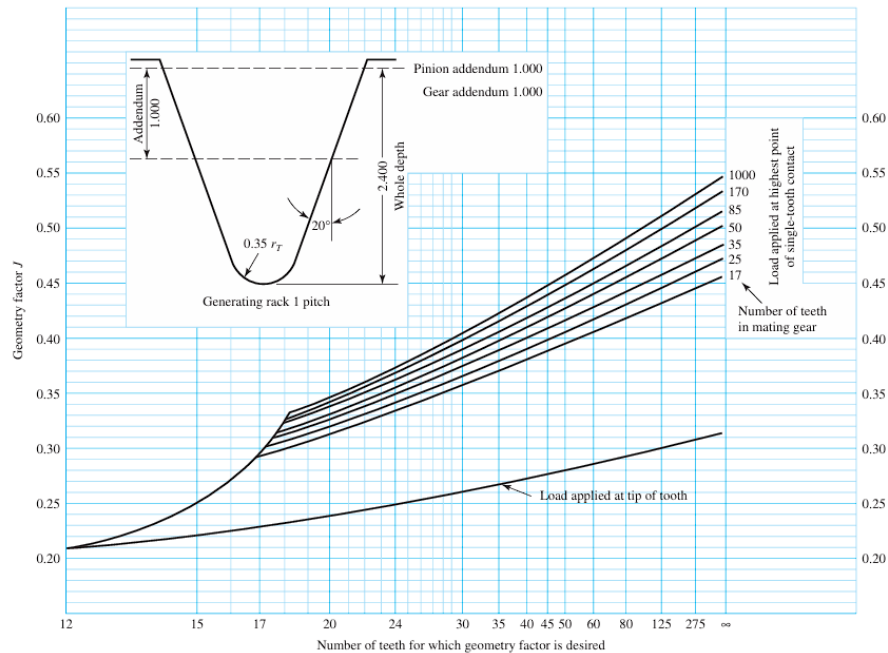


**Figure 13.** Spur Gear Geometry Factor

The number of pinion gears on the x-axis and the number of rack gears on the 18th curve axis are considered infinite, but since it is not shown infinitely on the graph, the highest value is evaluated.

$$Y_J = 0.33$$

**Allowable Bending Stress ( $S_t$ ):** It is the maximum stress value that a gear can safely withstand under bending stress on its teeth. This value is determined by considering the strength of the material and safety factors. [20]

Material AISI4140 and 197HB were taken [21]

| Material designation                                       | Heat treatment  | Minimum surface hardness <sup>1)</sup> | Allowable bending stress number <sup>2)</sup> , $s_{at}$ lb/in <sup>2</sup> |                                |               |
|--|---|--|---|--------------------------------|---------------|
|  |   |  | Grade 1   | Grade 2                        | Grade 3       |
| Steel <sup>3)</sup>  | Through hardened  | see figure 9                           | see figure 9  | see figure 9                   | --            |
|  | Flame <sup>4)</sup> or induction hardened <sup>4)</sup> with type A pattern <sup>5)</sup> | see table 8                            | 45 000  | 55 000                         | --            |
|  | Flame <sup>4)</sup> or induction hardened <sup>4)</sup> with type B pattern <sup>5)</sup> | see table 8                            | 22 000  | 22 000                         | --            |
|  | Carburized and hardened <sup>4)</sup>   | see table 9                            | 55 000  | 65 000 or 70 000 <sup>6)</sup> | 75 000        |
|  | Nitrided <sup>4)</sup> <sup>7)</sup> (through hardened steels)                            | 83.5 HR15N                             | see figure 10   | see figure 10                  | --            |
| Nitralloy 135M, Nitralloy N, and 2.5% Chrome (no aluminum) | Nitrided <sup>4)</sup> <sup>7)</sup>  | 87.5 HR15N                             | see figure 11   | see figure 11                  | see figure 11 |

**NOTES**

- <sup>1)</sup> Hardness to be equivalent to that at the root diameter in the center of the tooth space and face width.
- <sup>2)</sup> See tables 7 through 10 for major metallurgical factors for each stress grade of steel gears.
- <sup>3)</sup> The steel selected must be compatible with the heat treatment process selected and hardness required.
- <sup>4)</sup> The allowable stress numbers indicated may be used with the case depths prescribed in 16.1.
- <sup>5)</sup> See figure 12 for type A and type B hardness patterns.
- <sup>6)</sup> If bainite and microcracks are limited to grade 3 levels, 70,000 psi may be used.
- <sup>7)</sup> The overload capacity of nitrided gears is low. Since the shape of the effective S-N curve is flat, the sensitivity to shock should be investigated before proceeding with the design. [7]

Figure 14. Allowable Bending Stress Number for Steel Gear

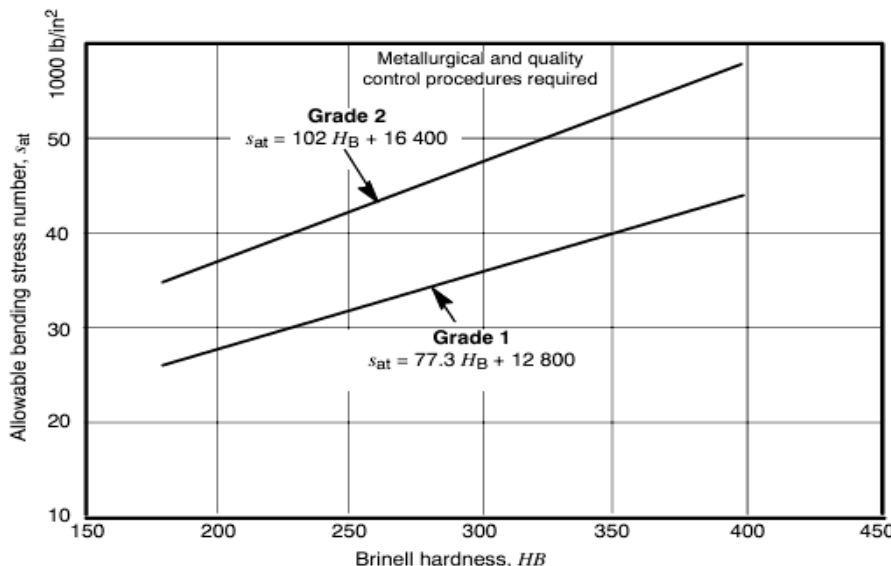


Figure 15. Allowable Bending Stress Number for Through Hardened Steel Gears

Small machine tools are generally through hardened and grade 1.

$$S_t = 77.3 \cdot 197 + 12800 = 77.3 \cdot 197 + 12800 = 28028.1 \text{ psi} = 193.25 \text{ MPa}$$

**Stress Cycle Factor Bending Stress ( $Y_N$  and  $Z_N$ ):** It is the fatigue life correction factor for bending stress. [15]

$$n = 60 \cdot L \cdot N \cdot q$$

**Number of Load Cycle (N):** It numerically indicates the number of times the gear teeth operate under load (rotation, contact, load carrying) throughout their life. [15]

**Life (L):** 2000 hours

**Speed (N):** 90 rev/min

**Number of Contact Per Revolution (Q):** 18 teeth

$$n = 60 \cdot 2000 \cdot 90 \cdot 18 = 194.4 \cdot 10^6$$

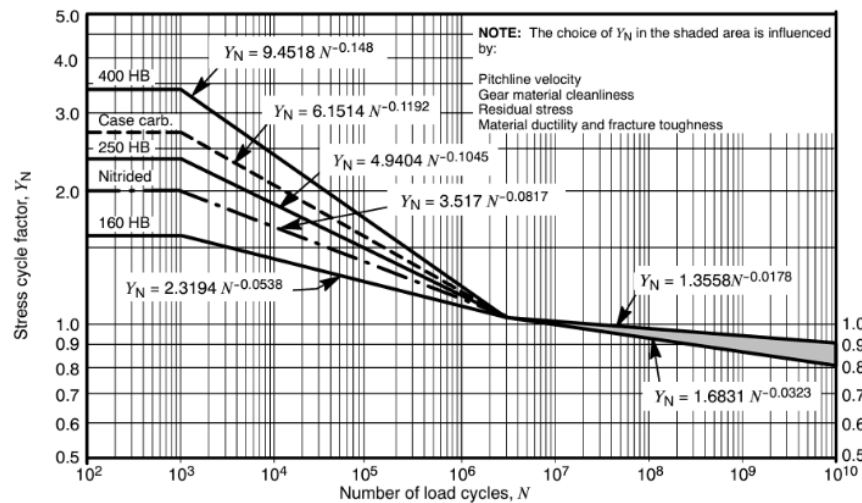


**Figure 16.** Bending Strength Stress Cycle Factor  $Y_N$

$$Y_N = 1.2$$

**Temperature Factor ( $Y_\theta$ ):** This is a factor that takes into account this effect, as the strength of the material decreases as the operating temperature increases. Operating the gear at high temperatures reduces its resistance, especially to bending stresses. [15]

$$Y_\theta = 1 \quad \text{if } T \leq 121^\circ\text{C}$$

**Reliability Factor ( $Y_Z$ ):** It is a safety correction factor that compensates for the decrease in fatigue strength of the gear at a certain reliability level. [15]

Reliability is 0.99 so  $Y_Z = 1$  [22]

**Elastic Coefficient ( $Z_E$ ):** It is the coefficient used to determine the Hertzian contact stress in gear contact. [15]

Elastic Coefficient  $C_p$  ( $Z_E$ ),  $\sqrt{\text{psi}}$  ( $\sqrt{\text{MPa}}$ ) Source: AGMA 218.01

| Pinion Material | Pinion Modulus of Elasticity $E_p$ , psi (MPa)* | Gear Material and Modulus of Elasticity $E_G$ , lbf/in <sup>2</sup> (MPa)* |   |   |  |  |   |
|-----------------|---|--|---|---|--|--|---|
|                 |   | Steel<br>$30 \times 10^6$<br>( $2 \times 10^5$ )                           | Malleable Iron<br>$25 \times 10^6$<br>( $1.7 \times 10^5$ ) | Nodular Iron<br>$24 \times 10^6$<br>( $1.7 \times 10^5$ ) | Cast Iron<br>$22 \times 10^6$<br>( $1.5 \times 10^5$ ) | Aluminum Bronze<br>$17.5 \times 10^6$<br>( $1.2 \times 10^5$ ) | Tin Bronze<br>$16 \times 10^6$<br>( $1.1 \times 10^5$ ) |
| Steel           | $30 \times 10^6$<br>( $2 \times 10^5$ )         | 2300<br>(191)  | 2180<br>(181)   | 2160<br>(179)   | 2100<br>(174)  | 1950<br>(162)  | 1900<br>(158)   |
| Malleable iron  | $25 \times 10^6$<br>( $1.7 \times 10^5$ )       | 2180<br>(181)  | 2090<br>(174)   | 2070<br>(172)   | 2020<br>(168)  | 1900<br>(158)  | 1850<br>(154)   |
| Nodular iron    | $24 \times 10^6$<br>( $1.7 \times 10^5$ )       | 2160<br>(179)  | 2070<br>(172)   | 2050<br>(170)   | 2000<br>(166)  | 1880<br>(156)  | 1830<br>(152)   |
| Cast iron       | $22 \times 10^6$<br>( $1.5 \times 10^5$ )       | 2100<br>(174)  | 2020<br>(168)   | 2000<br>(166)   | 1960<br>(163)  | 1850<br>(154)  | 1800<br>(149)   |
| Aluminum bronze | $17.5 \times 10^6$<br>( $1.2 \times 10^5$ )     | 1950<br>(162)  | 1900<br>(158)   | 1880<br>(156)   | 1850<br>(154)  | 1750<br>(145)  | 1700<br>(141)   |
| Tin bronze      | $16 \times 10^6$<br>( $1.1 \times 10^5$ )       | 1900<br>(158)  | 1850<br>(154)   | 1830<br>(152)   | 1800<br>(149)  | 1700<br>(141)  | 1650<br>(137)   |

**Figure 17.** Elastic Coefficient  $Z_E$

$$Z_E = 191\sqrt{\text{MPa}}$$

**Surface Condition Factor ( $Z_R$ ):** Depending on how smooth, even and high quality the gear surfaces are, the resistance to contact stresses increases or decreases. [15]

It is only used on pitting so it is 1.

**Allowable Contact Stress ( $S_c$ ):** It is the maximum contact stress that a material can withstand without permanent deformation or microcracks on its surface. [15]

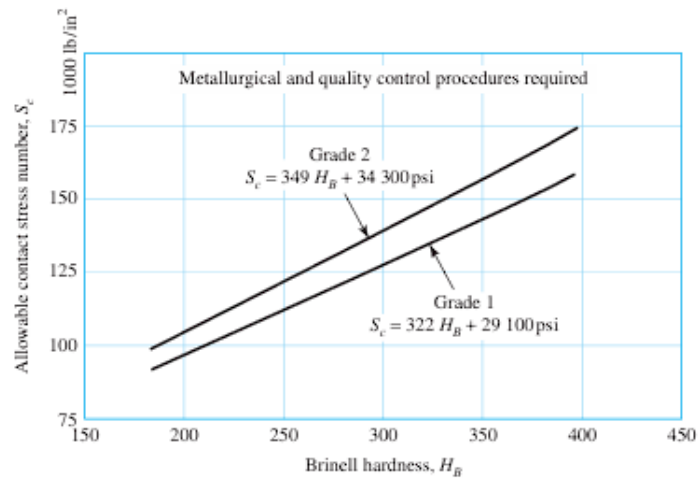


**Figure 18.** Contact Fatigue Strength for Through Hardened Steel Gears

$$S_C = 322H_B + 29100 = 322 \cdot 197 + 29100 = 92534 \text{ psi} = 638 \text{ MPa}$$

**Surface Strength Geometry Factor ( $Z_I$ ):** It is a coefficient that affects the surface contact strength depending on the geometry of the gear pair. It takes into account the effects of geometric factors such as tooth shape, module, gear ratio, and contact angle on the contact stress. (1)

$$Z_I = \frac{\cos\phi \cdot \sin\phi}{2m_N} \frac{m_G}{m_G + 1} = \frac{\cos\phi \cdot \sin\phi}{2m_N} \frac{(m_G + 1) - 1}{m_G + 1} = \frac{\cos\phi \cdot \sin\phi}{2m_N} \left[ 1 - \frac{1}{m_G + 1} \right]$$

**Load Sharing Ratio ( $m_N$ ):** It is the ratio that shows how the load is shared between the teeth when more than one tooth carries the load at the same time. Especially in helical gears, the teeth engage sequentially and thus the load is distributed to more than one tooth, which increases the strength. [15]

$$m_N = 1$$

**Speed Ratio ( $m_G$ ):** It is the value that shows the rotation speed ratio of the large gear (gear) to the small gear (pinion) in a gear pair. It is also defined by the ratio of the number of teeth. [15]

$$m_G = \frac{d_G}{d_P} = \frac{\infty}{18} = \infty$$

**Pressure Angle ( $\phi$ ):**  $20^\circ$

$$Z_I = \frac{\cos 20 \sin 20}{2} \left[ 1 - \frac{1}{\infty + 1} \right] = 0.16$$

**Hardness Ratio Factor ( $Z_w$ ):** It is coefficient that corrects the effect of the ratio between the hardnesses of the two materials in the gear pair on surface strength and contact stress. [15]

$$Z_w = 1 \quad \text{because of 2 material is same}$$

**Gear Bending Stress Equation:**

$$\sigma = W^t K_O K_V K_S \frac{K_H K_B}{b m_t Y_J} = 1333.32 \cdot 1.75 \cdot 1.03 \cdot 1 \frac{1.23 \cdot 1}{0.025 \cdot 0.0025 \cdot 0.33} \\ = 136.33 \text{ MPa}$$

**Bending Factor of Safety:**

$$S_F = \frac{S_t Y_N}{Y_\theta Y_Z \sigma} = \frac{193.25 \cdot 1.2}{1 \cdot 1 \cdot 136.33} = 1.70$$

**Gear Contact Stress Equation:**

$$\sigma_C = Z_E \sqrt{W^t K_O K_V K_S \frac{K_H Z_R}{d_{w_1} b Z_1}} = 191 \sqrt{1333.32 \cdot 1.75 \cdot 1.03 \cdot 1 \frac{1.17 \cdot 1}{0.045 \cdot 0.025 \cdot 0.16}} \\ = 754.91 \text{ MPa}$$

**Wear Factor of Safety:**

$$S_H = \frac{S_C Z_N Z_W}{Y_\theta Y_Z \sigma_C} = \frac{638 \cdot 1.2 \cdot 1}{1 \cdot 1 \cdot 754.91} = 1.02$$

### 3.4.2. Sheet Metal

**Maximum Bending Force (P):** The maximum bending force for a sheet metal part shaped on a press machine is the highest force applied to obtain the desired shape of the sheet metal. This force varies depending on the type of material, thickness, width of the sheet metal, how narrow the angle to be bent is, and how the bending process is performed. In particular, the force required to shape increases as the sheet metal gets thicker or when a harder material is used. In addition, the geometry of the die and punch used during the bending process - for example, v sharp or u sharp dies - directly affects the magnitude of this force. If very sharp corners are desired or a narrow die gap is used, higher force is required to shape the sheet metal. The correct calculation of this force is very important both in terms of ensuring that the sheet metal is shaped without damage and in order to prevent overloading of the press machine. Otherwise, tears, cracks in the sheet metal, or deformations in the mechanical components of the press may occur.

Therefore, the maximum bending force is a critical parameter that should be carefully evaluated in the press production process. [23]

$$P = \frac{k(UTS)LT^2}{W} = \frac{1.33 \cdot (430 \text{ N/mm}^2) \cdot (25 \text{ mm}) \cdot (1 \text{ mm})^2}{10 \text{ mm}} = 1430 \text{ N}$$

**Coefficient (k):** 1.33 for v-sharp die

**Ultimate tensile stress (UTS):** 430 MPa for copper alloy

**Length (L):** 25 mm

**Thickness (T):** 1 mm

**Open die (W):** 10 mm

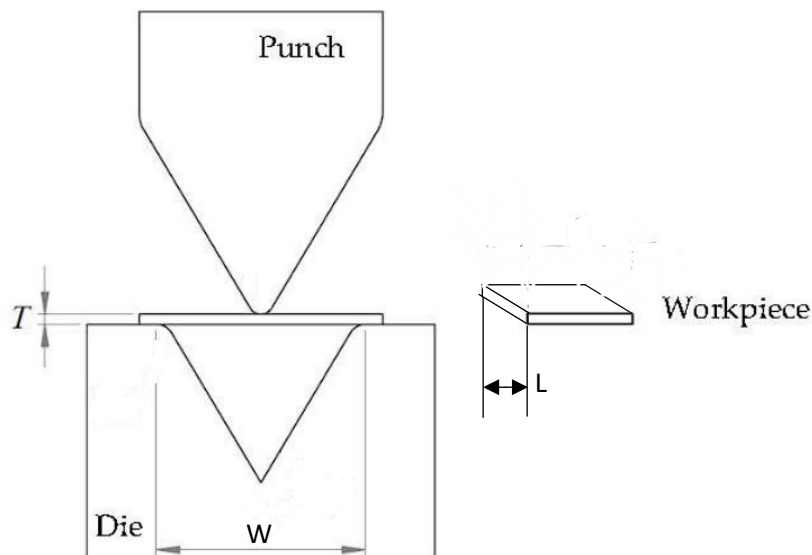


**Figure 19.** Parts of Press

**Springback:** It is the opening back of a sheet metal bent with a press after it comes out of the die, that is, the bending angle partially reverses. The reason for this phenomenon is that while the inner parts of the sheet change shape plastically during bending, the elastic deformation remaining in the outer parts recovers when the load is removed. Springback is especially more pronounced in thin and high-strength sheets. The sheet is bent with difficulty while in the die; however, when the die is opened, the sheet does not completely maintain its new shape and slightly returns to its old form. This situation increases the margin of error in production as it can cause deviations from the targeted angle. Therefore, engineers make corrections in the die design or bending angle by predicting the springback in advance. The main factors affecting the amount of

springback are the elasticity modulus of the sheet, yield strength, thickness, bending radius and the type of material used. As a result, springback is a natural and inevitable rebound behavior that should be taken into account in sheet metal forming processes. [24]

$$\begin{aligned}\frac{R_i}{R_f} &= 4\left(\frac{R_i \sigma_y}{ET}\right)^3 - 3\left(\frac{R_i \sigma_y}{ET}\right) + 1 \\ &= 4\left(\frac{3.6 \times 10^{-3} \cdot 280 \times 10^6}{150 \times 10^9 \cdot 1 \times 10^{-3}}\right)^3 - 3\left(\frac{3.6 \times 10^{-3} \cdot 280 \times 10^6}{150 \times 10^9 \cdot 1 \times 10^{-3}}\right) + 1 \\ &= 0.9798\end{aligned}$$

$$0.9798 \cdot 100 = 97.98 \rightarrow \%2.02$$

$$90^\circ \cdot \%2.02 = 1.82^\circ \rightarrow 88.18^\circ$$

Although the aim is 90 degrees when doing a v-press, the angle becomes 88.18 degrees with the springback.

**Von Mises:** It is a stress measure used to determine whether a material will undergo plastic deformation (permanent deformation). It is especially preferred to evaluate the behavior of ductile (plastically deformable) materials such as metals under complex loading. In reality, a material is often subjected to multi-axial stresses from different directions, not just one. The von Mises criterion reduces these multi-axial situations to a single "equivalent stress" value and compares this value with the yield strength of the material. If this equivalent stress exceeds the yield limit of the material, the material begins to deform plastically. [15]

**Maximum Bending Stress ( $\sigma_{max,bend}$ ):** It indicates the maximum bending stress and is the amount of normal stress at the point where the beam or similar element is most stressed under the effect of bending. This stress is the result of internal forces occurring within the elastic limits of the material. [15]

$$\sigma_{max,bend} = \frac{Mc}{I}$$

**Bending Moment (M):** It is the bending moment at that point; that is, it expresses the magnitude of the rotation effect created by the loads on the beam. The bending moment varies according to the cross-section of the beam. [15]

$$M = \frac{\sigma_y T^2 b}{4} = \frac{280 \text{ (N/mm}^2\text{)} \cdot (1 \text{ mm})^2 \cdot 25 \text{ mm}}{4} = 1750 \text{ Nmm}$$

**Distance From the Neutral Axis (C):** It is the distance between the neutral axis and the farthest point where the stress is maximum in the beam section; it can be thought of as the distance from the geometric center of the section to the end point, and as this distance increases, the stress also increases. [15]

$$c = \frac{T}{2} = \frac{1 \text{ mm}}{2} = 0.5 \text{ mm}$$

**Second-Area Moment (I):** It is the moment of inertia of the section and is calculated depending on the shape and size of the beam; this value indicates the resistance of the beam to bending. [15]

$$I = \frac{LT^3}{12} = \frac{25 \text{ mm} \cdot (1 \text{ mm})^3}{12} = 2.083 \text{ mm}^4$$

$$\sigma_{max,bend} = \frac{1750 \text{ Nmm} \cdot 0.5 \text{ mm}}{2.083 \text{ mm}^4} = 419.66 \text{ N/mm}^2 = 419.66 \text{ MPa}$$

**Maximum Shear Stress ( $\tau_{max}$ ):** It refers to the highest shear stress that occurs internally in a material or structural element. Shear stress occurs when different layers or parts of the material try to slide parallel to each other but in opposite directions. Maximum shear stress is especially important for the durability and safety of structures because materials generally have limiting resistances against shear stress and this type of stress can cause the material to deform or break. [15]

$$\tau_{max} = \frac{3V}{2A}$$

**Shear Force (V):** This is the force that passes through the section and creates a shear effect in the material. [15]

In this mechanism, the tangential force on the gear is the force acting on the sheet metal.

$$V = F_t = 1333.32 \text{ N}$$

## Area of Sheet Metal (A)

$$A = 50 \text{ mm} \cdot 1 \text{ mm} = 50 \text{ mm}^2$$

$$\tau_{max} = \frac{3V}{2A} = \frac{3F_t}{2A} = \frac{3 \cdot 1333.32 \text{ N}}{2 \cdot 50 \text{ mm} \cdot 1 \text{ mm}} = 40 \text{ N/mm}^2 = 40 \text{ MPa}$$

$$\sigma_{max} = \sqrt{\sigma_{max,bend}^2 + 3\tau_{max}^2} = \sqrt{419.66^2 + 3 \cdot 40^2} = 425.34 \text{ MPa}$$

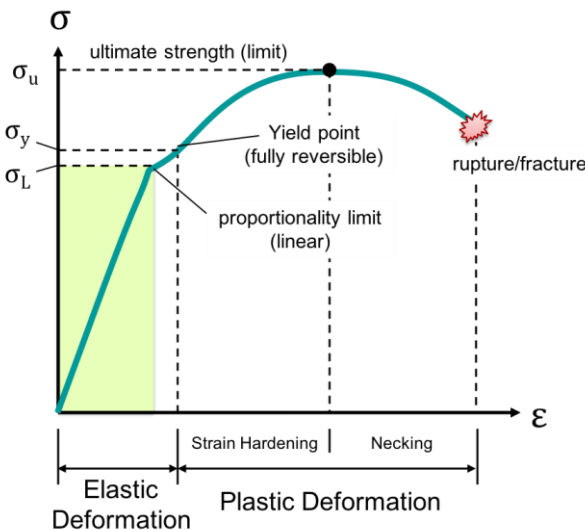


**Figure 20.** Stress-Strain Graphic

For the copper material, the yield stress was determined as 280 MPa and the ultimate tensile stress (UTS) as 430 MPa. In the von Mises stress analysis, the stress on the material was calculated as 425.34 MPa. This value is very close to the breaking strength of the material, and the material has now exceeded the elastic region limits and entered the plastic deformation region.

In the elastic region, the material returns to its original shape when the applied load is removed because the bonds between the atoms are deformed elastically and this deformation is reversible. However, under loads exceeding the yield strength, the material shows plastic deformation; in this process, the atoms permanently shift and the material continues to change shape. Plastic deformation causes permanent shape changes in the structure of the material and this deformation cannot be reversed.

As a result, the pressing process has caused the material to exceed its elastic limit and

enter the plastic deformation region, and a permanent shape change has occurred in the material. If the von Mises stress is very close to the breaking strength, it indicates that the material has exceeded the limits of safe use and precautions must be taken in such cases.

### 3.4.3. Buckling

*Johnson's critical load ( $P_{cr}$ ):* It is a method developed to more accurately represent the buckling behavior of short and intermediate-length columns. In such columns, buckling cannot be explained purely by elastic properties because the material begins to approach its yield point under load, showing signs of plastic deformation. Johnson addressed this by creating a model that considers both elastic and plastic behavior within the transition zone between purely elastic buckling and yielding. In this respect, Johnson's equation significantly differs from Euler's theory, which focuses solely on elastic buckling. Euler's formula is valid for long, slender columns where geometric instability dominates, and it assumes that the column buckles without experiencing any plastic deformation. However, in real-world engineering applications, most columns are neither extremely long nor extremely short, meaning their load-carrying capacity is influenced by both the material's strength and the column's geometry. Johnson's approach takes this complex interaction into account, offering safer and more realistic results. Therefore, while Euler's theory remains more theoretical and limited to specific conditions, Johnson's equation provides a practical solution for a wider range of column types encountered in structural design. For this reason, Johnson's formula is preferred for short and thick structural members, whereas Euler's formula is still applicable for very long and slender columns. [19]

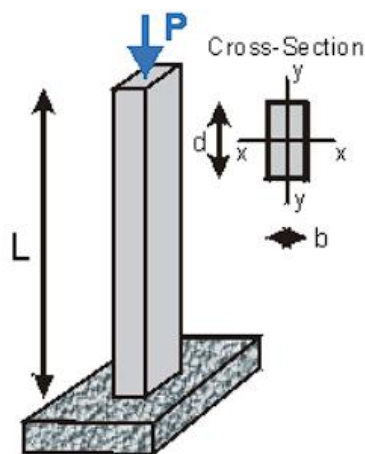


**Figure 21.** Cross Section of Box of Gear

$$P_{cr} = \sigma_y \cdot A \left[ 1 - \frac{\sigma_y}{4n \cdot \pi^2 \cdot E} (L/k)^2 \right]$$

**Elastic Modulus (E):** It is a mechanical property that indicates how much a material can stretch (deform) and then return to its original shape when stress is applied. It measures the hardness and elastic behavior of the material; materials with a high elastic modulus stretch less, meaning they are harder. [15]

$$E = 210 \text{ GPa} \text{ for AISI4140}$$

**End Fixity Coefficient (n):** The load carrying capacity of the column depends upon the condition of restraints at the two ends of the column. It is accounted by means of a dimensionless quantity called end fixity coefficient. [19]

**Table 5.** End Condition Table

| END CONDITION                      | N    |
|------------------------------------|------|
| BOTH END HINGED                    | 1    |
| BOTH END FIXED                     | 4    |
| ONE END FIXED AND OTHER END HINGED | 2    |
| ONE END FIXED AND OTHER END FREE   | 0.25 |

Since one edge of the box is connected to the body and the other edge is connected to the other edge of the box, in this mechanism one edge is fixed and the other edge is hinged.

$$n = 2$$

**Area (A):** Cross-section area

- b: 6 mm
- d: 205 mm

$$A = 6 \cdot 205 = 1230 \text{ mm}^2 = 1.23 \times 10^{-3} \text{ m}^2$$

**Yield Stress ( $\sigma_y$ )**

$$\sigma_y = 415 \text{ MPa} \text{ for AISI4140}$$

**Slenderness Ratio (L/k):** This is a dimensionless measure used to assess a column's or structural member's tendency to buckle based on its length relative to its cross-sectional properties. It is usually calculated as the effective length of the column divided by a key cross-sectional dimension, such as the radius of gyration. This ratio plays a crucial role in evaluating buckling risk: a higher slenderness ratio means a longer, thinner column that is more susceptible to buckling, while a lower ratio indicates a shorter, thicker column with greater resistance. In essence, the slenderness ratio is a key factor in understanding buckling behavior and ensuring safe, effective structural design. [19]

Length of the column (L)

$$L = 150 \text{ mm}$$

**Least Radius of Gyration of the Cross-Section About Its Axis (k):** It is a geometric property that expresses the resistance of a section to rotation about its weakest axis against buckling. It shows how the area of the section is distributed about that axis and affects the buckling strength.

$$k = \sqrt{I/A}$$

**Area Moment of Inertia (I):**

$$I = \frac{bd^3}{12}$$

$$I_x = \frac{6 \cdot 205^3}{12} = 4.31 \times 10^6 \text{ mm}^4$$

$$I_y = \frac{205 \cdot 6^3}{12} = 3690 \text{ mm}^4$$

$I_y$  is taken because it is small.

$$k = \sqrt{\frac{3690}{1230}} = 1.732 \text{ mm}$$

$$\text{Slenderness ratio} = \frac{L}{k} = \frac{150}{1.732} = 86.61$$

This ratio being less than 103.7 is proof that the Johnson equation should be used. 103.7 is an intermediate value for Euler and Johnson. Those greater than this value are solved with Euler and those smaller are solved with the Johnson equation.

$$P_{cr} = (415 \text{ N/mm}^2) \cdot (1230 \text{ mm}^2) \left[ 1 - \frac{415 \text{ N/mm}^2}{4 \cdot 2 \cdot \pi^2 \cdot (210000 \text{ N/mm}^2)} (86.61)^2 \right]$$

$$= 414.6 \text{ kN}$$

$$\sigma_{cr} = \frac{P_{cr}}{A} = \frac{414.6 \text{ kN}}{1230 \text{ mm}^2} = 337.1 \text{ MPa}$$

As a result of the analysis, the critical buckling force of the column was calculated as 414.6 kN. This critical force represents the maximum axial load that the column can carry without buckling. At the same time, the critical stress value was found to be 337.1 MPa. The critical stress indicates the highest stress level in the column section and reflects the material's approach to the buckling limit. These values are the basic parameters in determining the buckling strength of the column. If the load applied to the column exceeds the critical force, the column will be subjected to buckling and its structural stability will be compromised. Similarly, evaluating the critical stress according to the material's strength limits is important for safe design. Therefore, the loads to which the column will be exposed in engineering design must be kept below the critical force and stress values.

**Effective Length Factor (K):** It is the modified value of the actual length of a column depending on the boundary conditions affecting its buckling behavior. Depending on how the ends of the column are supported (e.g. both ends fixed, free, hinged, etc.), the column's buckling-resistant length will differ. The effective length coefficient is the adjustment of the actual length according to these boundary conditions and is used in buckling calculations. Thus, the column is modeled in the most appropriate way for its actual condition.

$$K = 2 \text{ because of 1 side fixed, 1 side free}$$

**b:** 6 mm

**d:** 205 mm

**L:** 150 mm

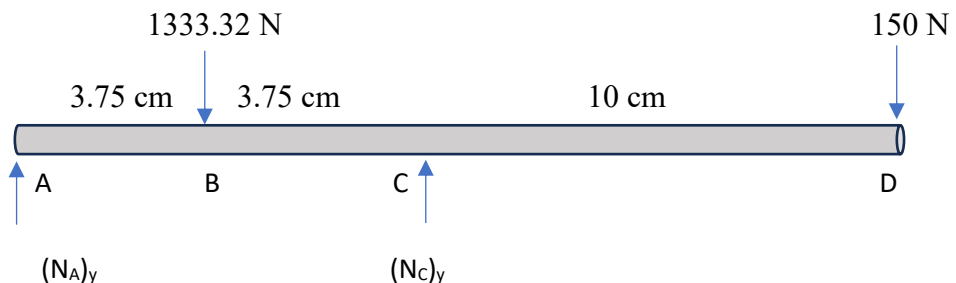
$$P_{cr} = \frac{\pi^2 \cdot (210 \times 10^9) \cdot (3690 \times 10^{-12})}{(2 \cdot 0.15)^2} = 84.98 \text{ kN}$$

$$\sigma_{cr} = \frac{P_{cr}}{A} = \frac{84.98 \times 10^3}{(6 \times 10^{-3}) \cdot (205 \times 10^{-3})} = 69.09 \text{ MPa}$$

As a result of the analysis, the critical buckling force of the column was calculated as 84.98 kN. This critical force represents the maximum axial load that the column can carry without buckling. At the same time, the critical stress value was found to be 69.09 MPa. The critical stress indicates the highest stress level in the column section and reflects the material's approach to the buckling limit. These values are the basic parameters in determining the buckling strength of the column. If the load applied to the column exceeds the critical force, the column will be subjected to buckling and its structural stability will be compromised. Similarly, evaluating the critical stress according to the material's strength limits is important for safe design. Therefore, the loads to which the column will be exposed in engineering design must be kept below the critical force and stress values.

### 3.4.4. Shaft

**Y-axis:**

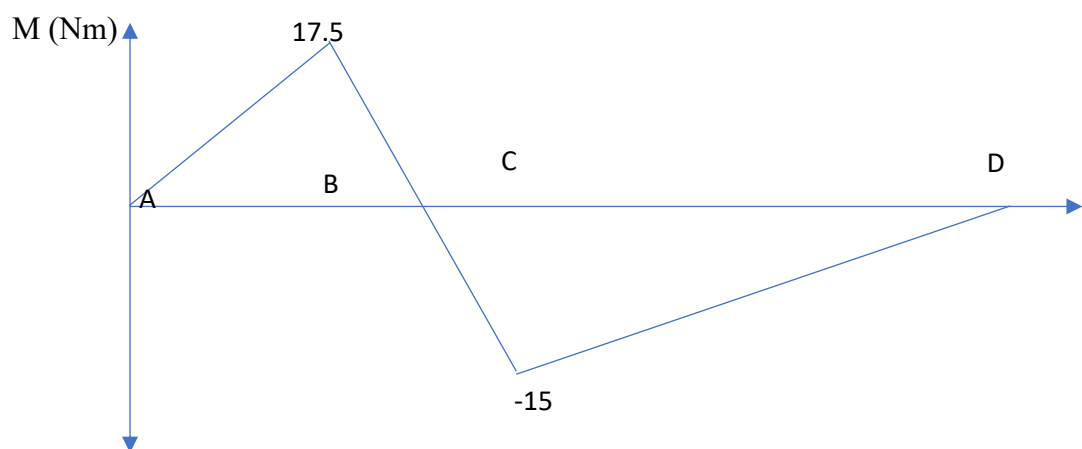
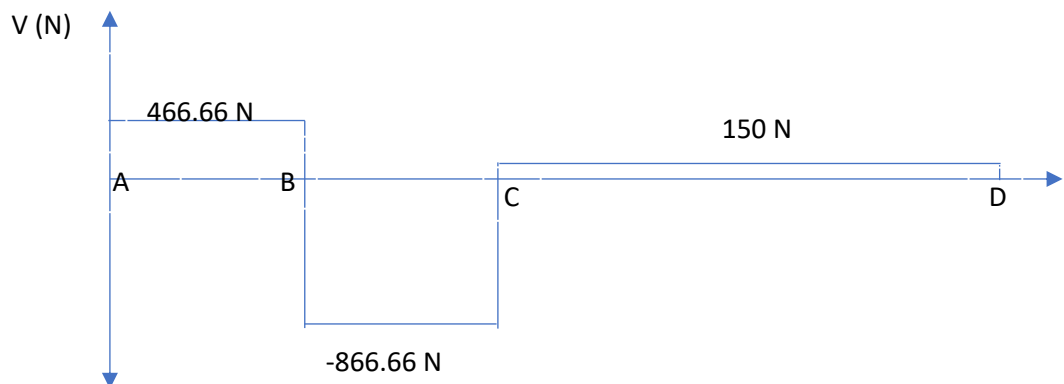


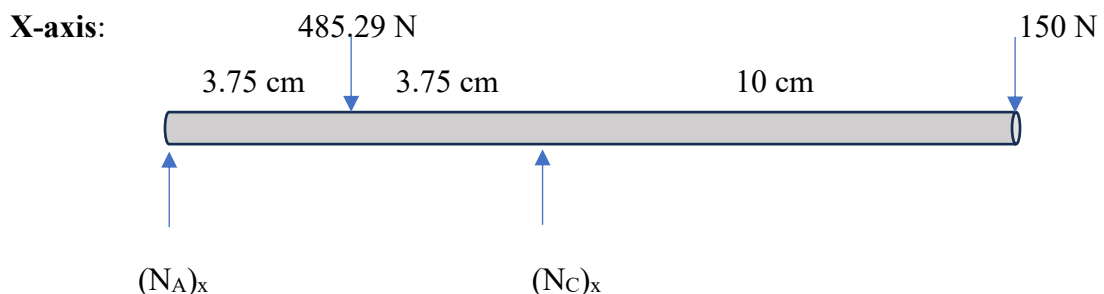
$$\sum (M_A)_y = 0 \rightarrow -1333.32 \cdot 3.75 - 150 \cdot 17.5 + (N_C)_y \cdot 7.5 = 0$$

$$\sum (M_D)_y = 0 \rightarrow 1333.32 \cdot 13.75 - (N_A)_y \cdot 17.5 - (N_C)_y \cdot 10 = 0$$

$$\sum F_y = 0 \rightarrow (N_A)_y + (N_C)_y - 150 - 1333.32 = 0$$

$$(N_A)_y = 466.66 \text{ N} \quad (N_C)_y = 1016.66 \text{ N}$$



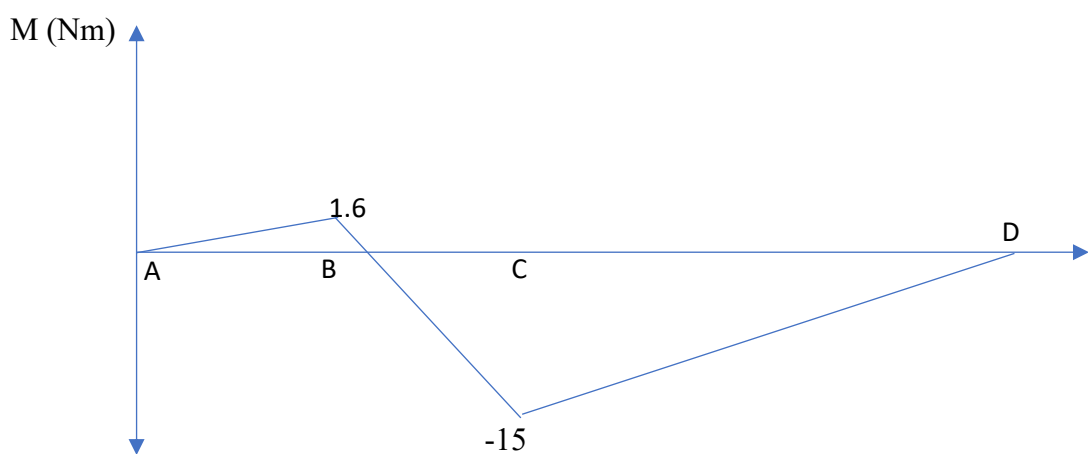
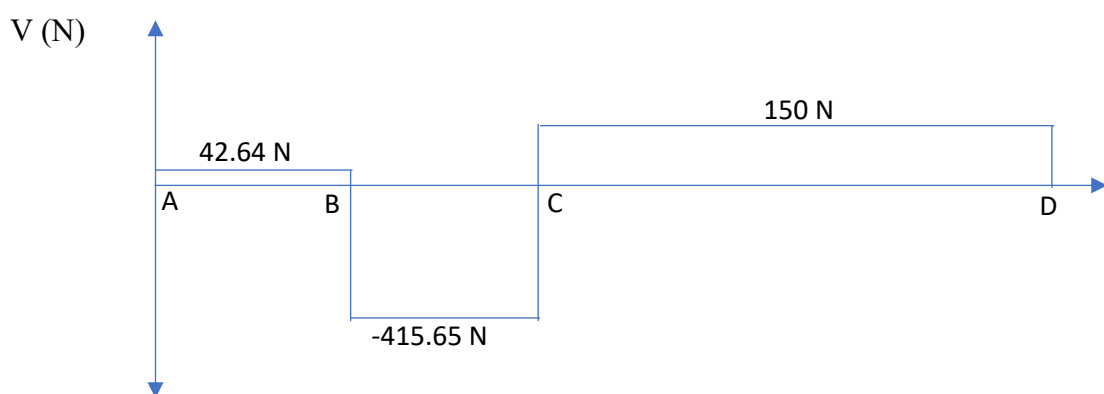


$$\sum (M_A)_x = 0 \rightarrow -485.29 \cdot 3.75 - 150 \cdot 17.5 + (N_C)_x \cdot 7.5 = 0$$

$$\sum (M_D)_x = 0 \rightarrow 485.29 \cdot 13.75 - (N_A)_x \cdot 17.5 - (N_C)_x \cdot 10 = 0$$

$$\sum F_x = 0 \rightarrow (N_A)_x + (N_C)_x - 150 - 485.29 = 0$$

$$(N_A)_x = 42.64 \text{ N} \quad (N_C)_x = 592.65 \text{ N}$$



$$N_A = \sqrt{(N_A)_x^2 + (N_A)_y^2} = \sqrt{42.64^2 + 466.66^2} = 468.61 \text{ N}$$

$$N_B = \sqrt{(N_B)_x^2 + (N_B)_y^2} = \sqrt{485.29^2 + 1333.32^2} = 1418.89 \text{ N}$$

$$N_C = \sqrt{(N_C)_x^2 + (N_C)_y^2} = \sqrt{592.65^2 + 1016.66^2} = 1176.79 \text{ N}$$

$$N_D = 150 \text{ N}$$

$$\sigma_A = \frac{N_A}{A} = \frac{468.61}{\pi \cdot 0.01^2} = 1.49 \text{ MPa} \quad \sigma_B = \frac{N_B}{A} = \frac{1418.89}{\pi \cdot 0.01^2} = 4.52 \text{ MPa}$$

$$\sigma_C = \frac{N_C}{A} = \frac{1176.79}{\pi \cdot 0.01^2} = 3.75 \text{ MPa} \quad \sigma_D = \frac{N_D}{A} = \frac{150}{\pi \cdot 0.01^2} = 477.46 \text{ kPa}$$

In cases where the exact direction of the 150 N force applied to the arm cannot be determined precisely, in order to calculate the maximum stresses on the shaft accurately and comprehensively, this force is accepted as 150 N separately and as a full value in both the x and y axes. This approach is preferred in order to eliminate the uncertainty regarding the direction of the force and to make a safe design by considering the most adverse loading conditions. In addition, the forces of the gear in the system in both the x and y axes are added to these values and the total force effect is calculated. In this way, in addition to the forces that each point on the shaft is exposed to, the bending moments created by these forces are determined in detail. This analysis method enables the safe calculation of the strength limits of the structural element even when the exact direction of the forces is not known and ensures that the shaft is protected against possible plastic deformation or fracture risks.

The  $N_A$ ,  $N_C$ ,  $\sigma_A$  and  $\sigma_C$  values do not exceed the critical force and critical stress limits in the analyses performed. This situation shows that a structural stability problem such as buckling will not occur on the box to which the shaft is connected. In addition, when the stresses formed at different points of the shaft are examined in detail, it is seen that these stresses are well below the yield strength of AISI 4140 steel, which is 280 MPa. Stress levels below the yield strength indicate that the material remains within elastic limits and that no permanent plastic deformation occurs. This means that the shaft will continue to

operate safely without any structural damage or permanent deformation under the loads on it. As a result, both the mechanical strength and structural stability of the shaft have been ensured under current loading conditions, and the system is expected to function safely for a long time.

## 4. SIMULATION SETUP

In this section, the aim is to numerically investigate the U and V-type bending operations performed using the handcrafted press brake machine developed within the scope of the project. To validate the experimental applications in a virtual environment and to analyze structural behaviors in greater detail, ANSYS Workbench software was utilized. Through the analyses conducted in ANSYS, critical parameters such as stresses, deformations, plastic strains, and the springback effect encountered during the sheet metal bending process were observed.

The simulations were carried out using die and sheet geometries modeled to match the experimental setup, with accurate material definitions and contact conditions. In this way, not only was the accuracy of the physical tests evaluated, but it also became possible to make predictions for similar sheet forming applications in a digital environment and to plan the process more efficiently.

### 4.1. Geometry and Modeling

The first step of the simulation process for the bending operations conducted in this study was the creation of the die geometries used in the physical system. The die set was designed in three dimensions using SolidWorks, ensuring that the dimensions precisely matched those of the manufactured tools. These designs were then transferred to the ANSYS environment in STEP format.

The sheet metal geometry, being the main element subjected to deformation during the operation, was created directly within the ANSYS Discovery environment. This approach allowed the dimensions and positioning of the sheet to be flexibly defined according to simulation requirements. All prepared geometries were imported into the ANSYS Workbench platform and combined within a Static Structural model to form the complete simulation setup.

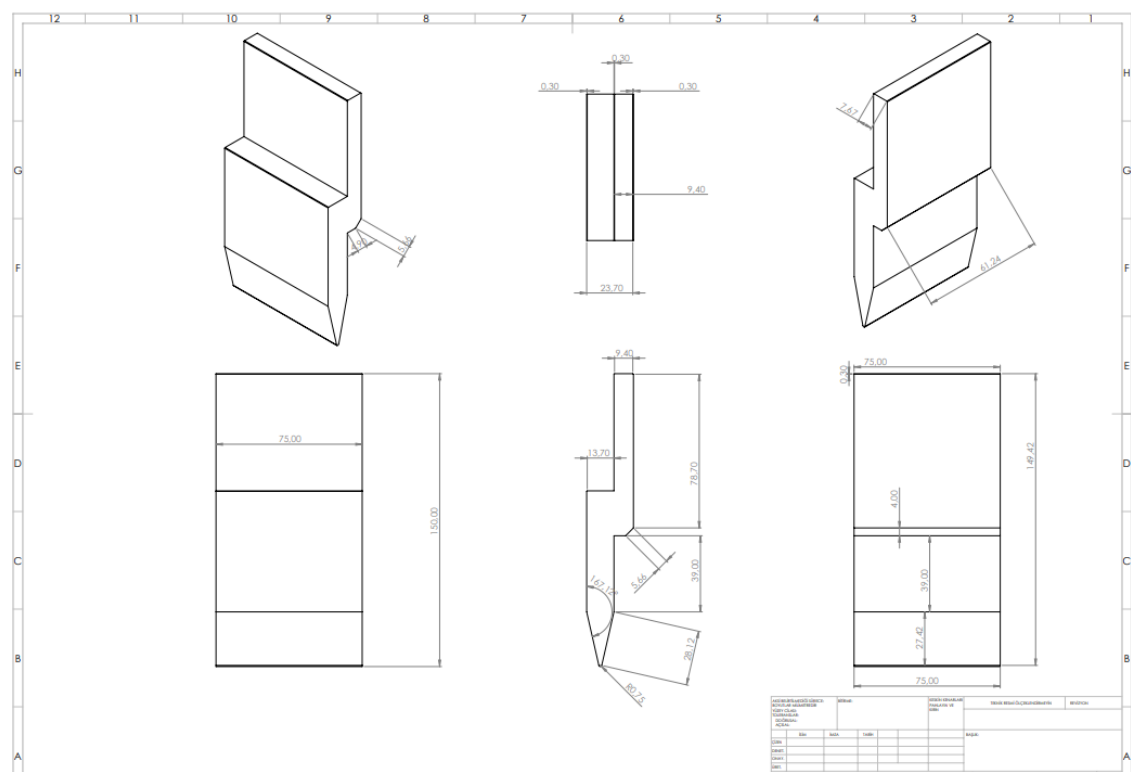


**Figure 22.** Upper Die Technical Drawing

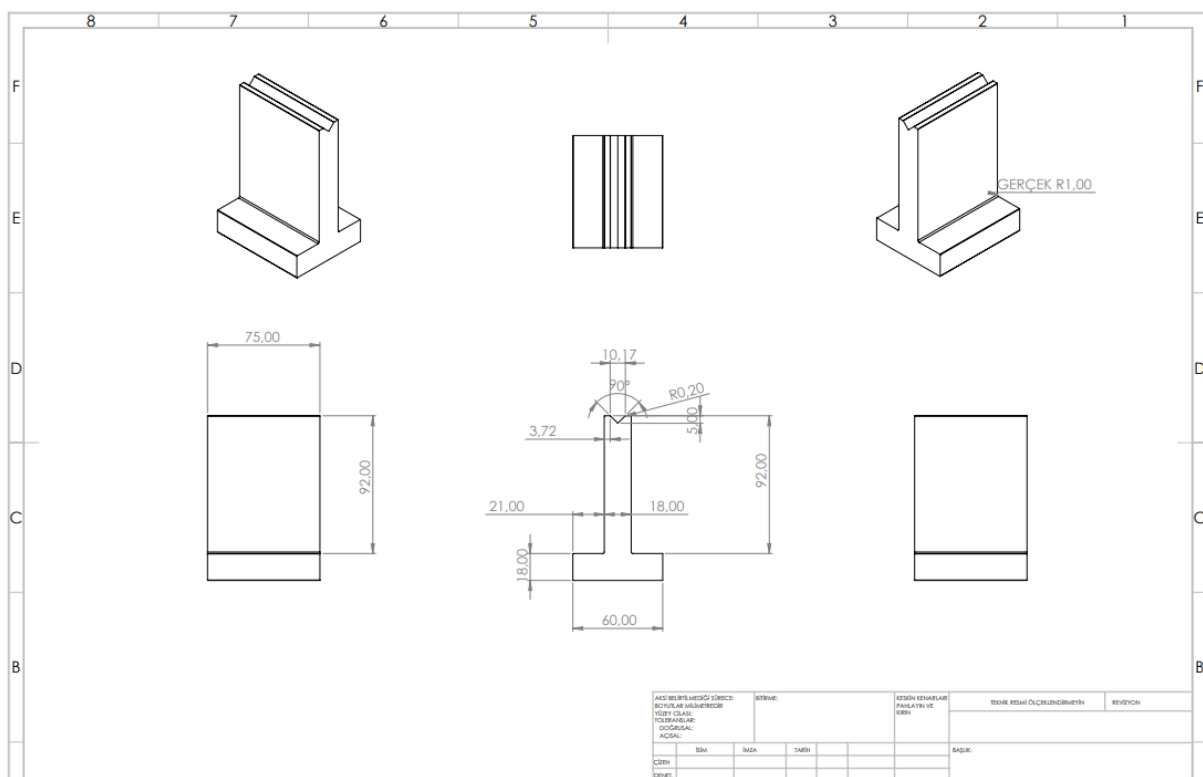


**Figure 23.** Lower Die Technical Drawing

## 4.2. Simulation and Results

### 4.2.1. U-Bending Analysis – Step 1

In this section, the analysis of the U-bending process performed with the press brake was carried out using the displacement method in ANSYS. The simulation was applied to a sheet metal part with dimensions of 1 mm × 25 mm × 50 mm, using two separate press tools. The die opening and the target bend angles were both set to 90 degrees.

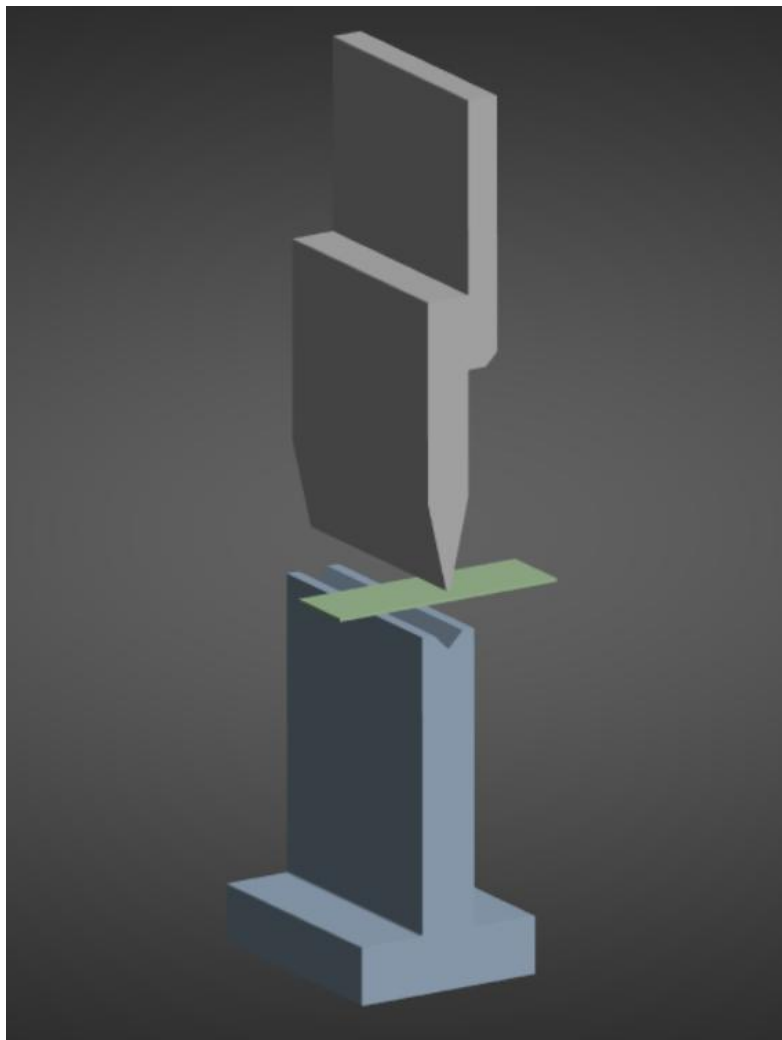


**Figure 24.** Sheet Metal and Dies in ANSYS Discovery

| Details of "Analysis Settings" |                    |
|--------------------------------|--------------------|
| <b>Step Controls</b>           |                    |
| Number Of Steps                | 10,                |
| Current Step Number            | 10,                |
| Step End Time                  | 10, s              |
| Auto Time Stepping             | Program Controlled |
| <b>Solver Controls</b>         |                    |
| Solver Type                    | Direct             |
| Weak Springs                   | Off                |
| Solver Pivot Checking          | Program Controlled |
| Large Deflection               | On                 |
| Inertia Relief                 | Off                |
| Quasi-Static Solution          | Off                |
| <b>Rotordynamics Controls</b>  |                    |
| <b>Restart Controls</b>        |                    |
| <b>Nonlinear Controls</b>      |                    |
| Newton-Raphson Option          | Program Controlled |
| Force Convergence              | Program Controlled |
| Moment Convergence             | Program Controlled |
| Displacement Convergence       | Program Controlled |
| Rotation Convergence           | Program Controlled |
| Line Search                    | Program Controlled |
| Stabilization                  | Constant           |
| --Method                       | Energy             |
| --Energy Dissipation Ratio     | 0,1                |
| --Activation For First Substep | No                 |
| --Stabilization Force Limit    | 0,2                |

**Figure 25.** U Bending Step 1 Analysis Settings

This image shows various simulation parameters within the “Analysis Settings” window. A time-dependent (transient) analysis is conducted, with a total simulation time of 10 seconds divided into 10 steps (Number of Steps: 10). The analysis is solved using a Direct solver, and large deformations are considered (Large Deflection: On). Inertia effects (Inertia Relief) and quasi-static solution methods (Quasi-Static Solution) are disabled. Additionally, weak springs are not used, and various convergence criteria (force, moment, displacement, rotation convergence) are monitored by the software to handle the nonlinear behavior of the system. For stabilization, the “Energy”-based method is selected, with a damping ratio of 0.1 and a force limit of 0.2. These settings are specifically used to improve the stability and accuracy of the solution in simulations involving contact and large deformations. The same settings will also be applied in Step 2 of the simulation.

#### 4.2.1.1. Material Definitions

For the sheet metal, "Copper Alloy" was selected from the ANSYS material library. Since the dies are defined as rigid bodies, no material assignment was made for them. The elastic and plastic properties of the material are provided in the accompanying figure.

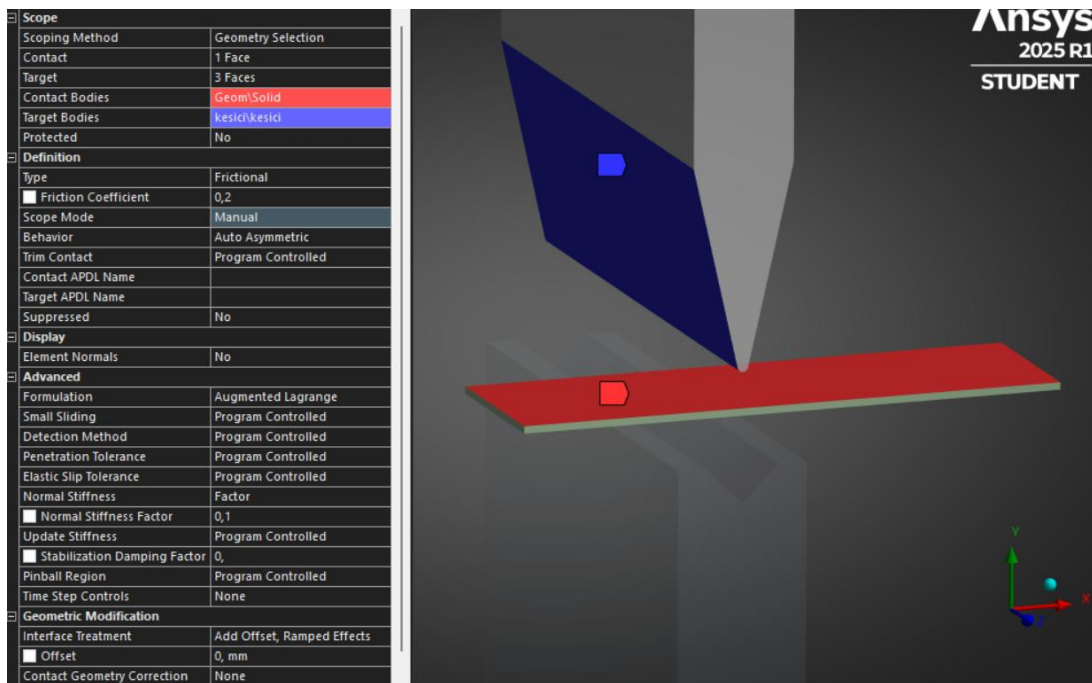
| Structural  |                                     |
|---|-------------------------------------|
| <b>▼ Isotropic Elasticity</b>                     |                                     |
| Derive from                                       | Young's Modulus and Poisson's Ratio |
| Young's Modulus                                   | 1,1e+05 MPa                         |
| Poisson's Ratio                                   | 0,34000                             |
| Bulk Modulus                                      | 1,1458e+05 MPa                      |
| Shear Modulus                                     | 41045 MPa                           |
| Isotropic Secant Coefficient of Thermal Expansion | 1,8e-05 1/°C                        |
| Compressive Ultimate Strength                     | 0 MPa                               |
| Compressive Yield Strength                        | 280,00 MPa                          |
| Tensile Ultimate Strength                         | 430,00 MPa                          |
| Tensile Yield Strength                            | 280,00 MPa                          |

Figure 26. Copper Alloy Material Definitions

#### 4.2.1.2. Assembly and Contact Settings

After all parts were imported into the Static Structural module in ANSYS Workbench, the assembly process was carried out. The parts were aligned as follows:

- The sheet metal was positioned in two separate steps, respectively.
- The upper and lower dies were aligned concentrically.



**Figure 27.** Contact Setting of Upper Die

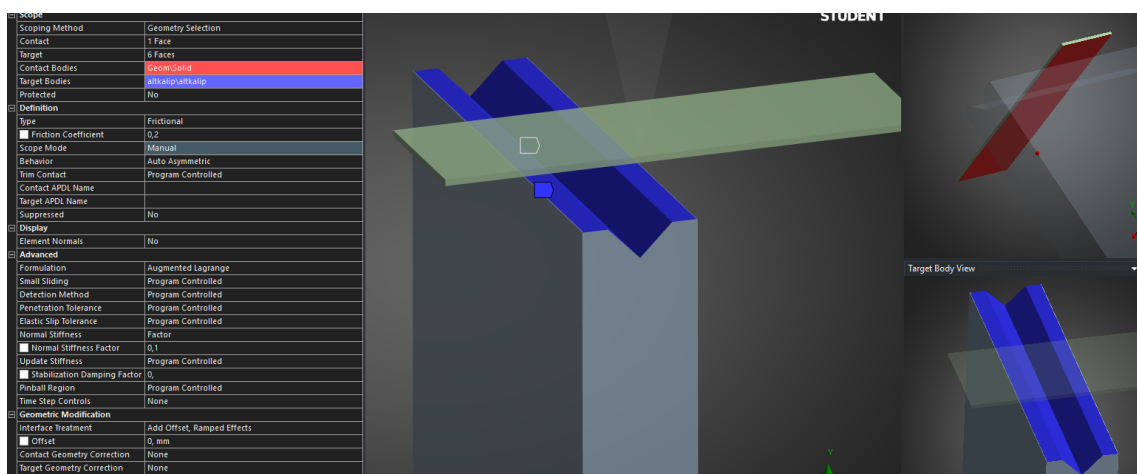


**Figure 28.** Contact Setting of Lower Die

In these figures, the contact settings defined in ANSYS Mechanical have been configured appropriately for a sheet bending analysis. The contact type has been selected as Frictional, and the coefficient of friction between the contact surfaces has been set to 0.2. The basis for selecting a friction coefficient of 0.2 lies in values commonly recommended in the literature for sheet metal forming processes. For bending operations conducted under unlubricated or lightly lubricated conditions, a coefficient of friction in the range of 0.1 to 0.3 is typically used. Therefore, the value of 0.2 is considered a balanced and suitable choice for both realistic contact modeling and maintaining solution stability.

The contact behavior and orientation have been set to Auto Asymmetric, allowing for more stable contact formation. The contact formulation is defined as Augmented Lagrange, which accurately calculates contact forces and permits a small amount of penetration, thereby ensuring both a stable and flexible solution. The Normal Stiffness Factor is set to 0.1, making the contact appear softer to reduce numerical difficulties during the solution. The stabilization damping coefficient is defined as 0, meaning that no additional damping is applied to the system.

In the Interface Treatment section, the “Add Offset, Ramped Effects” option has been activated. This allows the contact to begin at zero separation and gradually engage during the simulation. As a result, sudden force spikes and contact errors are prevented.

#### 4.2.1.3. Mesh Settings

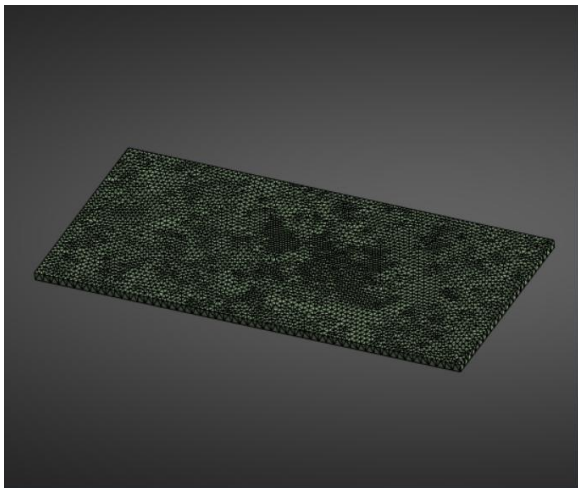


**Figure 29.** Meshed Sheet

| Details of "Patch Conforming Method" - Method |                    |
|---|--------------------|
| <b>Scope</b>                                  |                    |
| Scoping Method                                | Geometry Selection |
| Geometry                                      | 1 Body             |
| <b>Definition</b>                             |                    |
| Suppressed                                    | No                 |
| Method  | Tetrahedrons       |
| Algorithm                                     | Patch Conforming   |
| Element Order                                 | Use Global Setting |
| <b>Advanced Improve Options</b>               |                    |
| Aggressive Thin Face Collapse                 | Program Controlled |
| Automatic Node Movement                       | Program Controlled |
| <b>Refinement Options</b>                     |                    |
| Refine at Thin Section                        | No                 |

**Figure 30.** Patch Conforming Method Settings

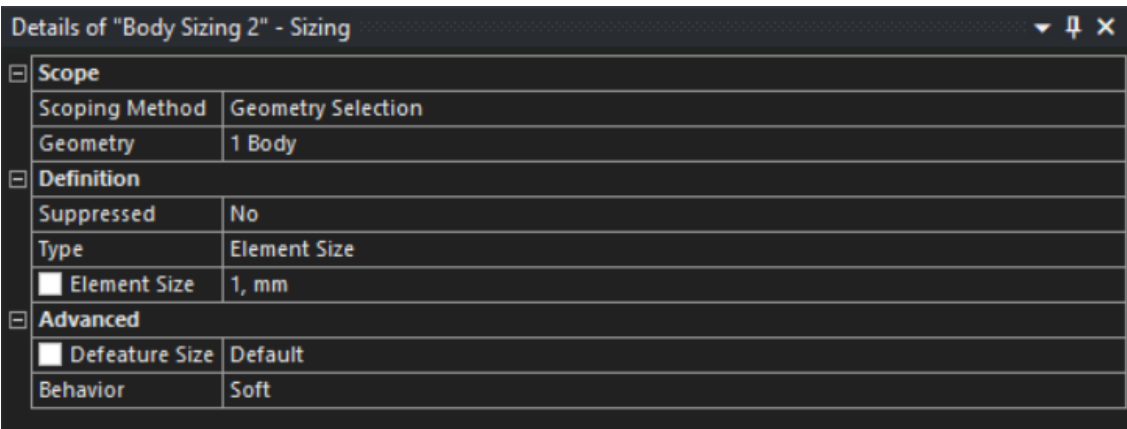


**Figure 31.** Body Sizing Settings



**Figure 32.** Face Sizing Settings

In these figures, the mesh settings used in ANSYS are shown in detail. In the first image, Tetrahedron elements were selected as the mesh type using the Patch Conforming Method.

In the second image, a general Body Sizing was applied to the solid body, and the element size was set to 1 mm.

In the third image, Face Sizing was applied to the top surface, and the element size was defined as 0.6 mm. This setting was used to generate a finer mesh structure on surfaces requiring more precise solutions, such as contact regions.

#### 4.2.1.4. Boundary Conditions

The simulation was carried out in two separate processes, each consisting of three steps:

- **Loading** (the die moves downward)
- **Unloading** (the die moves upward)

- **Springback** (the springback effect is observed)

**Upper Die:** Displacement is applied first in the -Y direction from the 0 position, and then in the +Y direction.

|    | Steps | Time [s] | <input checked="" type="checkbox"/> X [mm] | <input checked="" type="checkbox"/> Y [mm] | <input checked="" type="checkbox"/> Z [mm] |
|----|-------|----------|--|--|--|
| 1  | 1     | 0,       | 0,   | 0,   | 0,   |
| 2  | 1     | 1,       | 0,   | -0.5                                       | 0,   |
| 3  | 2     | 2,       | = 0,                                       | = -2.875                                   | = 0,                                       |
| 4  | 3     | 3,       | = 0,                                       | = -5.25                                    | = 0,                                       |
| 5  | 4     | 4,       | = 0,                                       | = -7.625                                   | = 0,                                       |
| 6  | 5     | 5,       | = 0,                                       | -10,                                       | = 0,                                       |
| 7  | 6     | 6,       | = 0,                                       | = -8,                                      | = 0,                                       |
| 8  | 7     | 7,       | = 0,                                       | = -6,                                      | = 0,                                       |
| 9  | 8     | 8,       | = 0,                                       | = -4,                                      | = 0,                                       |
| 10 | 9     | 9,       | = 0,                                       | = -2,                                      | = 0,                                       |
| 11 | 10    | 10,      | = 0,                                       | 0,   | = 0,                                       |

**Figure 33.** Upper Die Displacement Settings

**Lower Die:** Movement is restricted in all axes.

|    | Steps | Time [s] | <input checked="" type="checkbox"/> X [mm] | <input checked="" type="checkbox"/> Y [mm] | <input checked="" type="checkbox"/> Z [mm] |
|----|-------|----------|--|--|--|
| 1  | 1     | 0,       | = 0,                                       | = 0,                                       | = 0,                                       |
| 2  | 1     | 1,       | 0,   | 0,   | 0,   |
| 3  | 2     | 2,       | = 0,                                       | = 0,                                       | = 0,                                       |
| 4  | 3     | 3,       | = 0,                                       | = 0,                                       | = 0,                                       |
| 5  | 4     | 4,       | = 0,                                       | = 0,                                       | = 0,                                       |
| 6  | 5     | 5,       | = 0,                                       | = 0,                                       | = 0,                                       |
| 7  | 6     | 6,       | = 0,                                       | = 0,                                       | = 0,                                       |
| 8  | 7     | 7,       | = 0,                                       | = 0,                                       | = 0,                                       |
| 9  | 8     | 8,       | = 0,                                       | = 0,                                       | = 0,                                       |
| 10 | 9     | 9,       | = 0,                                       | = 0,                                       | = 0,                                       |
| 11 | 10    | 10,      | = 0,                                       | = 0,                                       | = 0,                                       |

**Figure 34.** Lower Die Displacement Settings

**Sheet Metal:** Fixed along the Z-axis at its side edges. Free to move along the X and Y axes.

|    | Steps | Time [s] | <input checked="" type="checkbox"/> Z [mm] |
|----|-------|----------|--|
| 1  | 1     | 0,       | = 0,                                       |
| 2  | 1     | 1,       | 0,   |
| 3  | 2     | 2,       | = 0,                                       |
| 4  | 3     | 3,       | = 0,                                       |
| 5  | 4     | 4,       | = 0,                                       |
| 6  | 5     | 5,       | = 0,                                       |
| 7  | 6     | 6,       | = 0,                                       |
| 8  | 7     | 7,       | = 0,                                       |
| 9  | 8     | 8,       | = 0,                                       |
| 10 | 9     | 9,       | = 0,                                       |
| 11 | 10    | 10,      | = 0,                                       |

**Figure 35.** Sheet Metal Displacement Settings

#### 4.2.1.5. Results

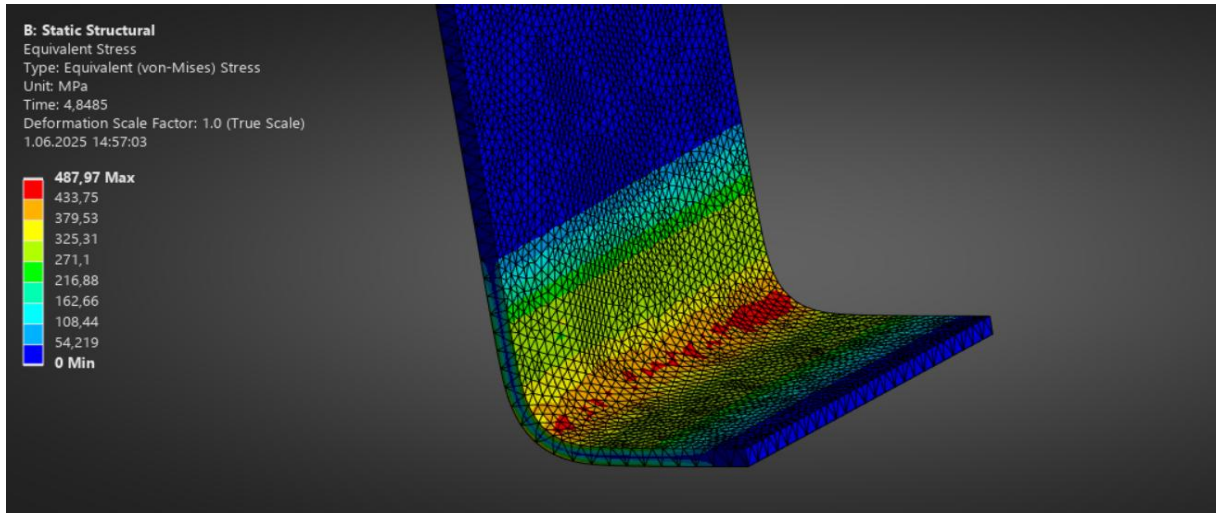


**Figure 36.** Maximum Press Moment in Step 1

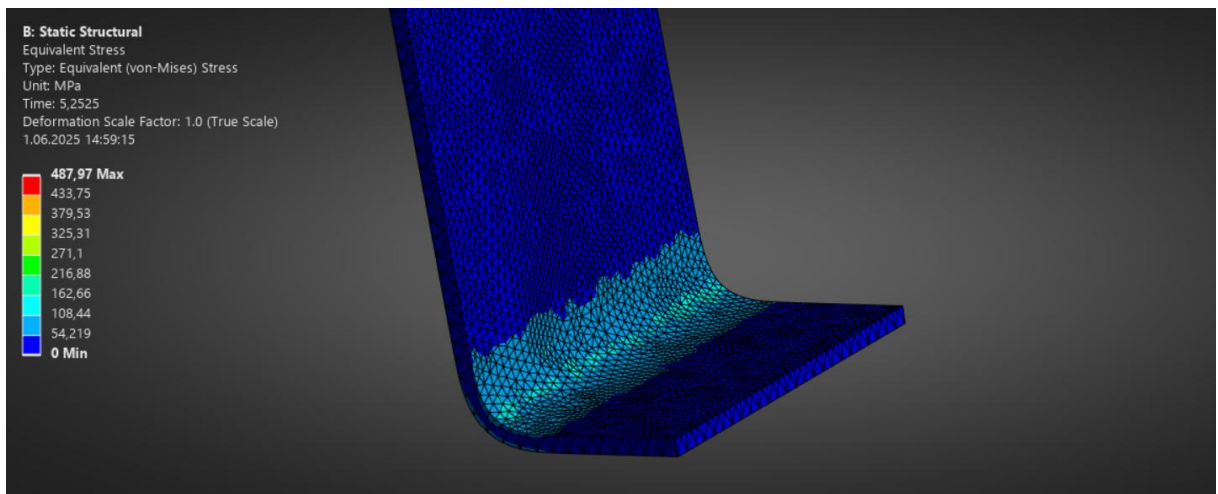


**Figure 37.** The First Moment the Press is Released from the Workpiece in Step 1

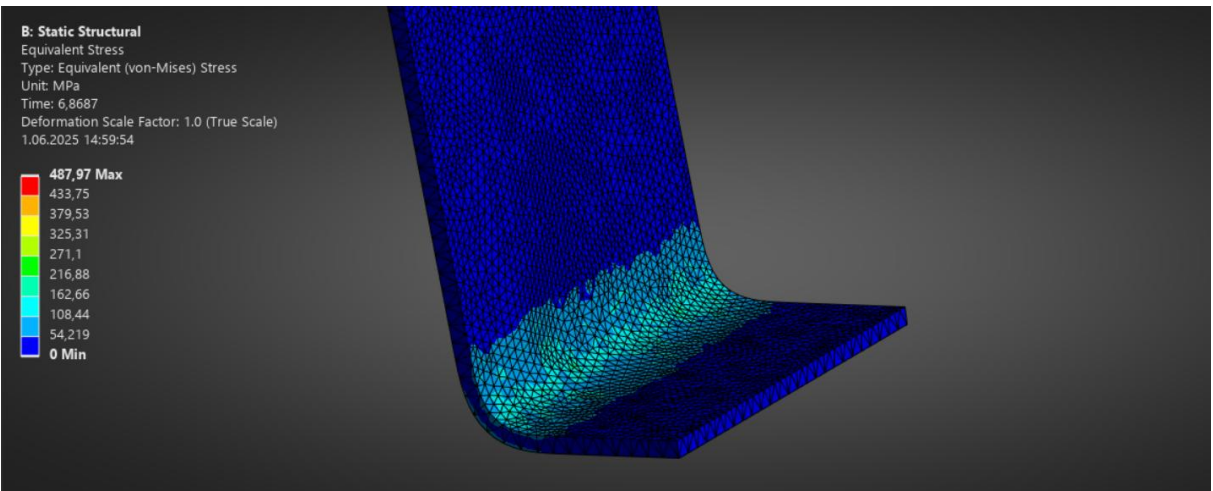


**Figure 38.** Final State After Springback in Step 1

In the first image, the equivalent stresses (von Mises) in the part reach their maximum level at the moment when the die applies the highest force, with a peak value observed at 487.97 MPa. The intense red regions, especially around the bent corner, indicate the areas where the material is most severely strained. In the second image, the force applied by the die has been removed—meaning the die has started to move upward. At this moment, the stresses have rapidly decreased, though there are still residual internal forces present within the part. The third image shows the state of the fully unloaded and released part, that is, its condition after springback. At this stage, an angular opening of approximately 1.9° has occurred in the material. Additionally, the stresses are no longer concentrated only at the corner, but have spread across a wider area.

#### 4.2.2. U Bending – Step 2

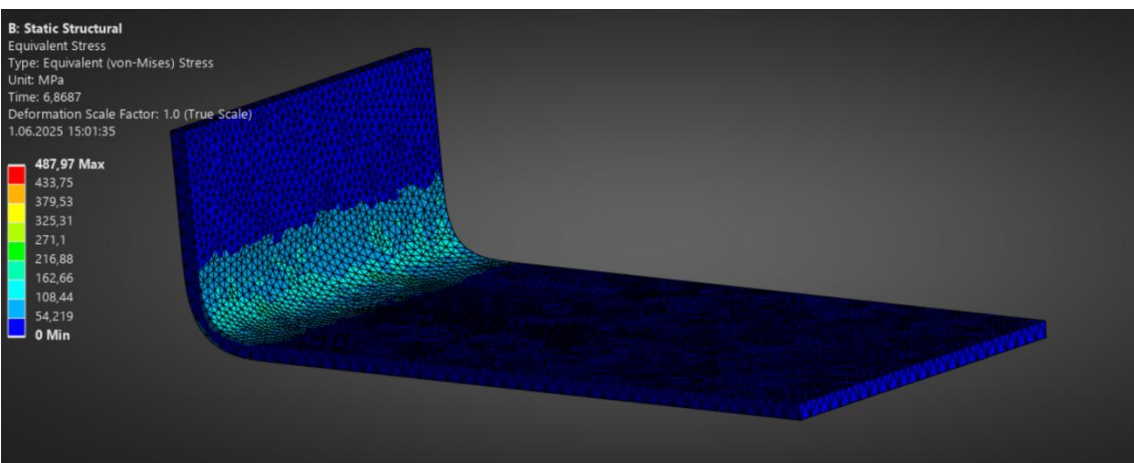


**Figure 39.** End of the First Step of U Bending

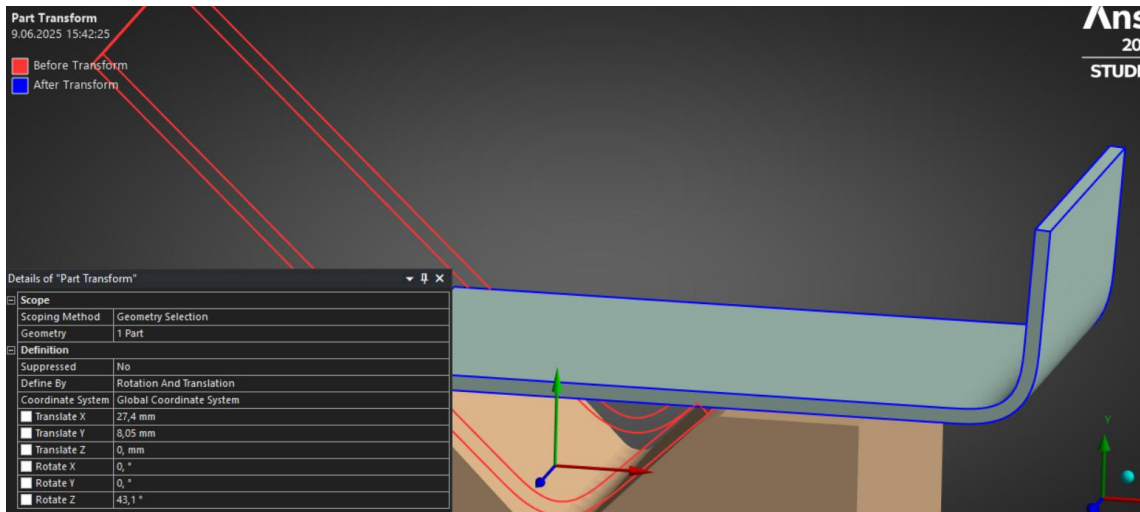


**Figure 40.** Part Transform Settings

In the first image, the initial bending phase of the two-step U-bending analysis has been completed, and the equivalent stress distribution of the part is shown. The left end of the part has been successfully bent, and the springback effect has been observed. In the second image, the preparation of this bent part for the second bending step using the “Part Transform” command in ANSYS Mechanical is demonstrated. The part has been translated along the X-axis from the left side to allow pressing from that direction. Although the part was theoretically intended to be positioned at a  $90^\circ$  interval, due to the springback effect from the first step, it was rotated by  $43.1^\circ$  instead of  $45^\circ$  for alignment. This slight angle deviation results from the material’s elastic recovery and was considered to ensure proper positioning of the second bending. Except for a change in contact settings (which will be explained in the next section), all other settings have been preserved as in the first step.

#### 4.2.2.1. Contact Settings

These settings largely resemble the contact definitions used in the first step. The only difference is the change made to the “**Interface Treatment**” option between the bottom die and the part, which has been set to “**Adjust to Touch**.” This choice was made as a precaution against small gaps that may form between surfaces due to the “**Part Transform**” command used to rotate and reposition the part after the first bend.

The “**Adjust to Touch**” setting automatically eliminates such gaps and initiates the contact, ensuring that the simulation runs accurately and stably. All other parameters remain the same as in the first step: **frictional contact, friction coefficient of 0.2,**

## Augmented Lagrange formulation, and Auto Asymmetric contact behavior.

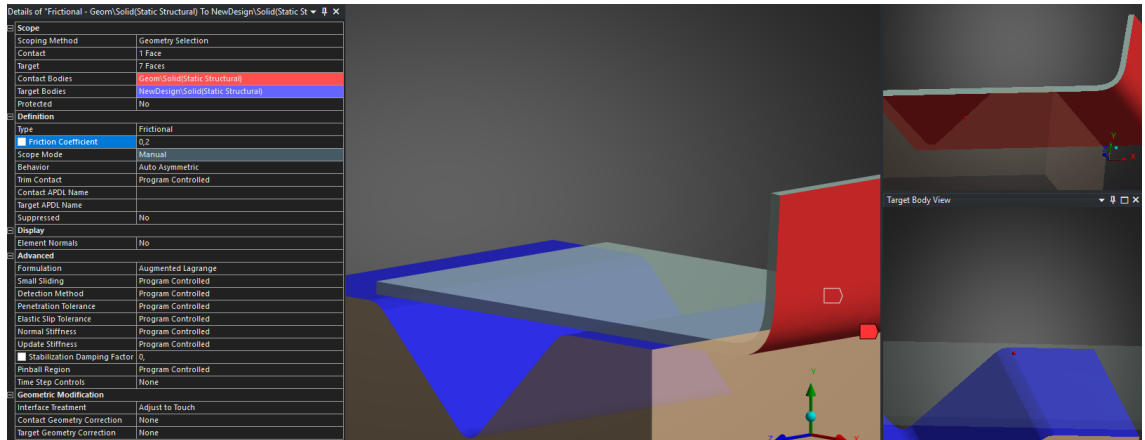


**Figure 41.** Contact Setting of Step 2

### 4.2.2.2. Results

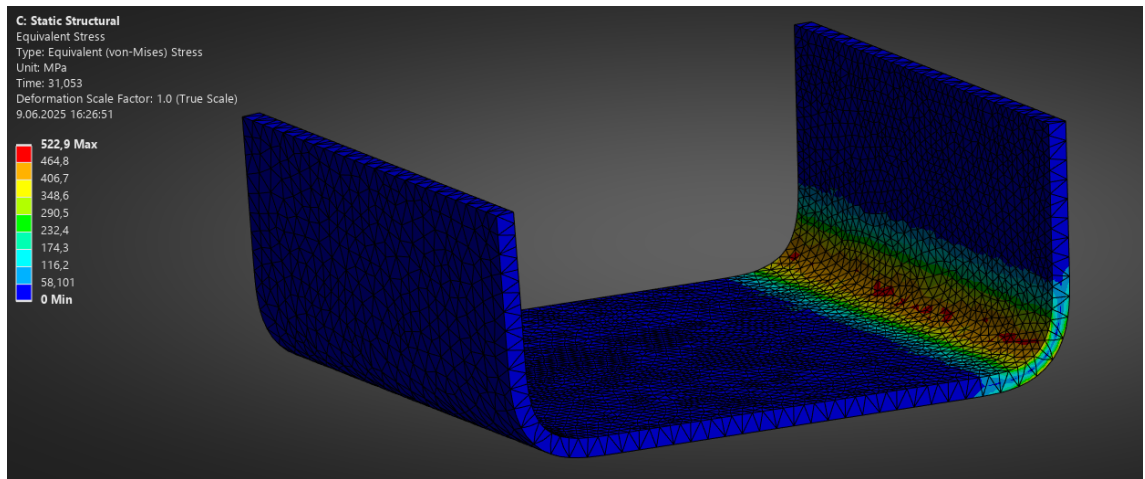


**Figure 42.** Maximum Press Moment in Step 2

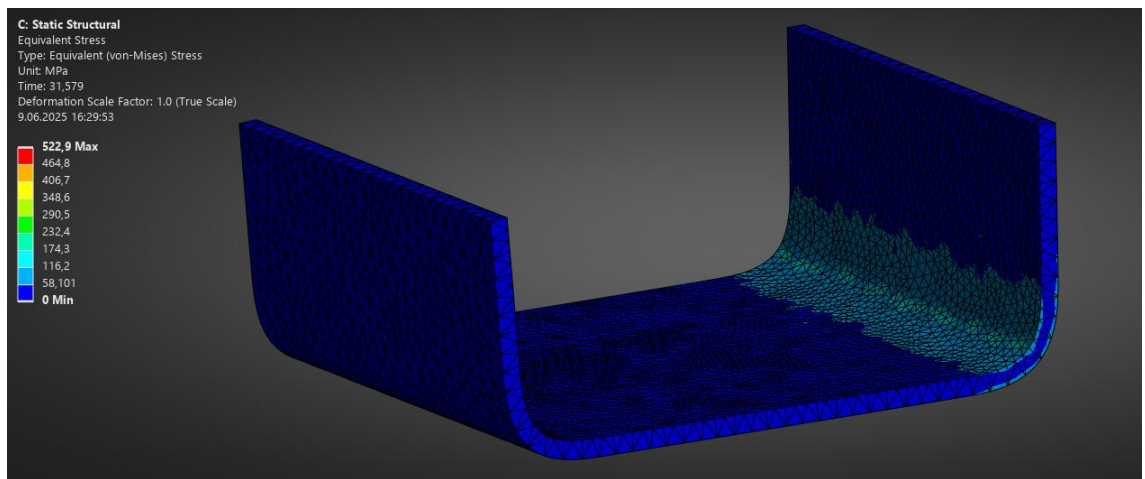


**Figure 43.** The First Moment the Press is Released from the Workpiece in Step 2

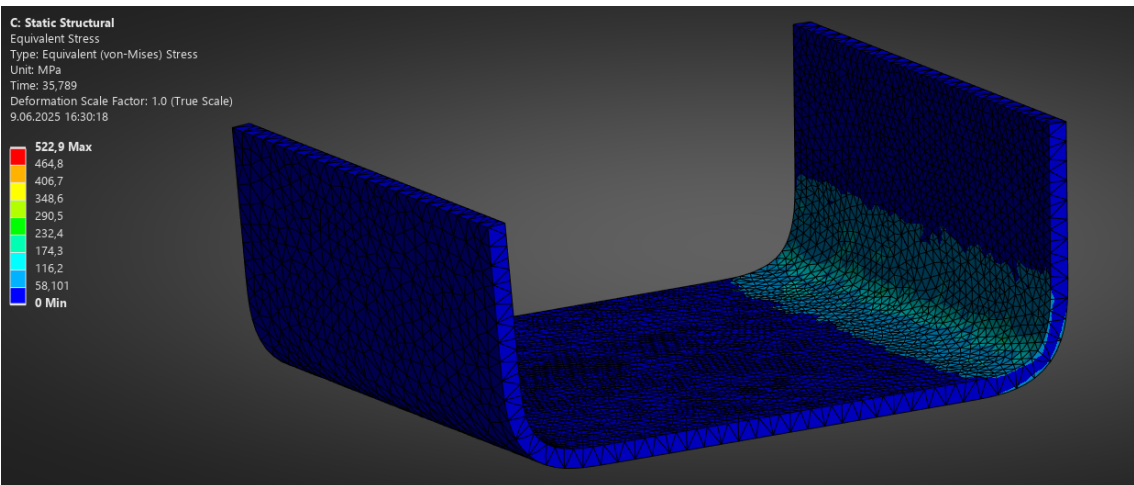


**Figure 44.** The Final State After Springback in Step 2

In the first image, the equivalent stresses (von-Mises) occurring in the part at the moment when the die applies the maximum force are observed, reaching a peak value of 522.9 MPa. The stresses are particularly concentrated in the right corner region where the second bend takes place.

In the second image, the die begins to move upward, separating from the part, and a decrease in stress values has begun.

The third image shows the springback state after the load has been completely removed. At this stage, a noticeable springback has occurred in the bending region of the part, and the stresses have spread over a wider area. The simulation has been completed.

#### 4.2.3. V-Bending Analysis

In this section, the analysis of the V-bending process performed using the press brake was conducted on a sheet metal with dimensions of 1 mm × 25 mm × 50 mm, previously created in ANSYS. The bending was applied precisely at the center of the sheet using the displacement method. The die opening and, consequently, the target angle were set to 90 degrees.

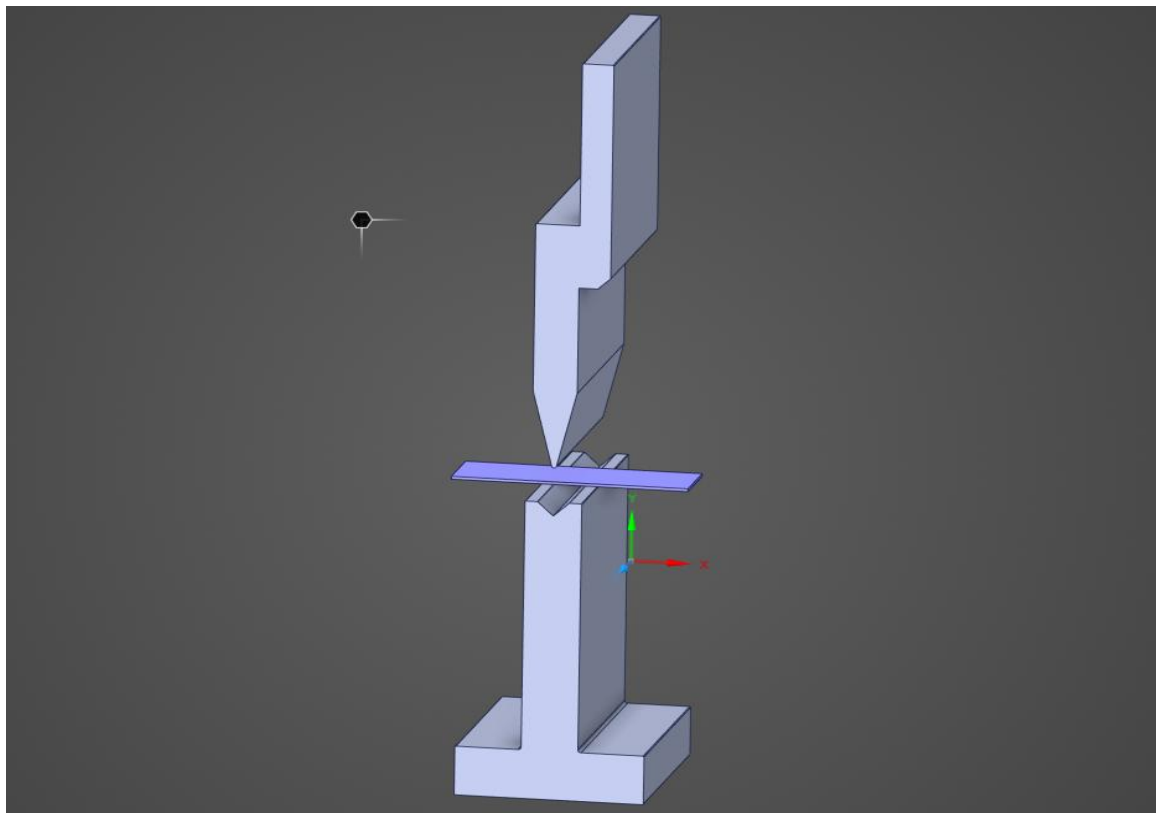


**Figure 45.** Placement of the Sheet Metal into the Die for V-Bending

#### 4.2.3.1. All Analysis Settings

The settings used in this analysis are exactly the same as those applied in the first step of the two-step U-bending process. Consistency was ensured by using the same mesh method, contact definitions, solution controls, and material behavior. In particular, accurately reflecting the material–die interaction through contact settings and maintaining the same coefficient of friction contributed to improved reliability between the analyses by preserving solution stability.

#### 4.2.3.2. Results

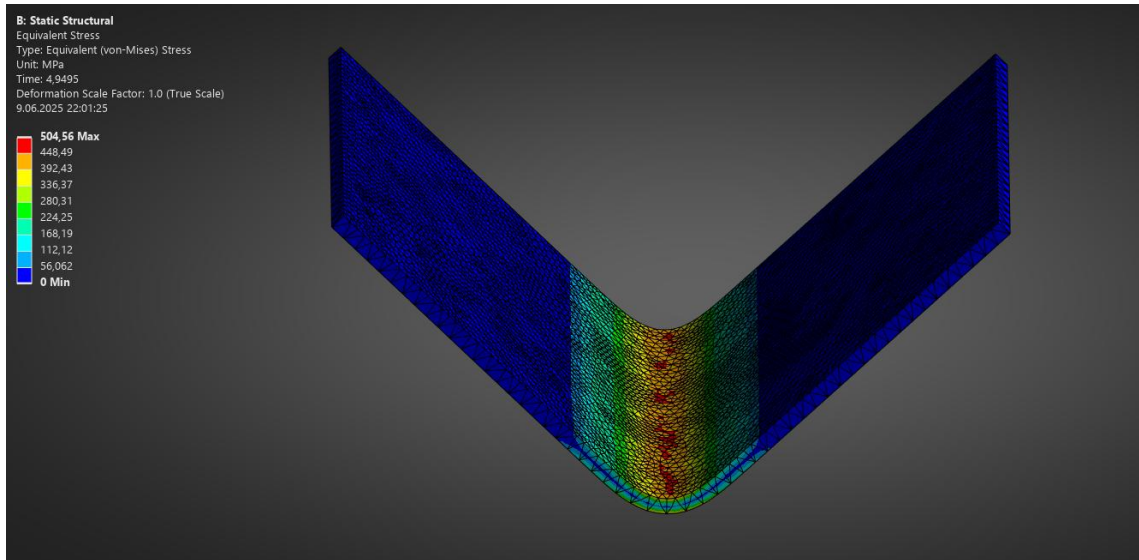


**Figure 46.** Maximum Press Moment in V Bending

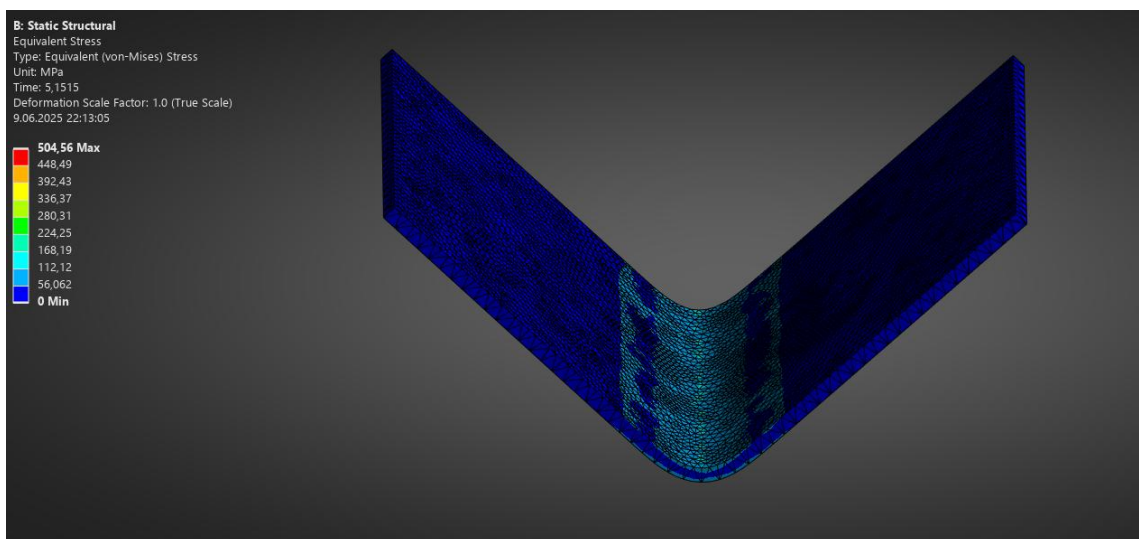


**Figure 47.** The First Moment the Press is Released from the Workpiece in V Bending

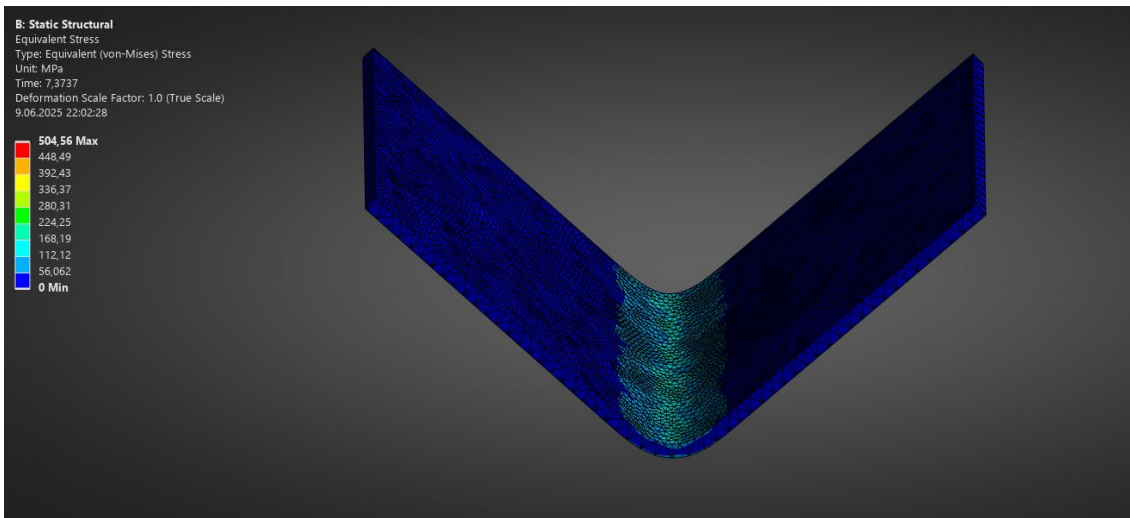


**Figure 48.** Final State After Springback in V Bending

The first image captures the moment when the punch applies maximum force, with the equivalent stress in the part reaching its peak at 504.56 MPa. The stress is particularly concentrated in the central area where the die makes contact. The second image shows the initial moment when the press begins to retract; at this point, the stresses start to decrease but remain present. The third image illustrates the final state of the part after springback. At this stage, an angular opening of approximately 1.9° has again occurred. The stress distribution has spread from the center toward a broader area, and while the part largely retains its V-shape, the springback effect is clearly observable.

#### 4.3 General Evaluation

When the U and V bending analyses are evaluated in general, it is observed that a consistent and comparable simulation environment was established by using the same analysis settings and contact parameters for both processes. The equivalent stress values obtained during the moment of maximum press force reached 504.56 MPa and were heavily concentrated in the bent regions. In both types of bending, a springback-induced angular recovery of approximately 1.9° was observed, clearly demonstrating the effect of elastic springback on post-bending shape deformation. In U bending, stress concentrations occurred at two separate corners, whereas in V bending, the stress was concentrated in the center. All these results, when compared with the manually calculated theoretical values, will demonstrate the accuracy of the analyses and provide important insights into the reliability of the design. Thus, the agreement between the numerical simulations and the theoretical approach forms a strong data set that supports the

engineering validity of the conducted study.

## 5. RESULTS & DISCUSSION

Within the scope of this study, the developed manual mini press brake device was thoroughly tested through both experimental and numerical methods. For the bending operations carried out using V and U-type dies, 1 mm thick C11000 copper alloy sheets were used. In the V-die application performed on specimens prepared with a width of 25 mm, the targeted 90° bending angle was theoretically calculated as 88.18°, corresponding to approximately 1.82° of springback. When simulated in ANSYS Workbench, a result of 88.1° was obtained, showing only a 0.08° deviation from the theoretical value. Since the U-type bending involved applying the V-type operation twice, the same springback values were observed. In the ANSYS simulation, the maximum von Mises stress in the copper sheet was measured as 504.56 MPa, which significantly exceeds the yield strength of 280 MPa and clearly indicates plastic deformation. The theoretical value for the same stress was calculated as 425.34 MPa. The 15.7% difference between these values is attributed to the displacement-based loading method used in ANSYS, which does not apply a linear force.

The maximum theoretical bending force was calculated as 1.43 kN. To produce this force manually, a torque of approximately 30 Nm was required. In the mechanism with a lever arm of 0.2 m, this corresponds to an applied hand force of about 150 N. In the stress analysis of the gear mechanism made of AISI 4140 steel, the von Mises stress under a 425 MPa load was evaluated.

Within the buckling analysis, the device's column carrier was evaluated using the Johnson formula. For a column length of 150 mm, the critical buckling load was calculated as 84.98 kN, and the corresponding critical stress as 69.09 MPa. The forces applied at points A and C were 468.61 N and 1176.79 N, respectively, both significantly below the critical load, indicating that no buckling is expected to occur. These results, when considered with a slenderness ratio below Euler's critical threshold, confirm the appropriateness of using the Johnson formula.

In the shaft calculations, the system's behavior under load was analyzed in both x and y directions. The maximum shear force on the shaft occurred at point B with a value of

1418.89 N, resulting in a stress of 4.52 MPa. Compared to AISI 4140's yield strength, these results show that no bending will occur on the shaft.

## 6. CONCLUSION

In light of the presented results, the developed manual press brake device has successfully achieved its targeted performance in terms of both mechanical strength and functionality. Despite being manually operated, the device demonstrated high precision, with only about a 2% deviation in the bending process. The difference in springback observed between the V and U-type bending processes clearly reflects the effect of die geometry on deformation distribution. The theoretical von Mises stress of 425.34 MPa confirms that the material exceeded its yield strength and underwent plastic deformation, validating the occurrence of permanent shape change. This also indicates that the device can generate the required energy density for effective bending.

The approximately 150 N of applied force through the handle mechanism demonstrates the device's ergonomic suitability. In the gear system analysis, the 425 MPa stress experienced remained just under the 430 MPa yield limit of AISI 4140 steel, suggesting that the gears can endure long-term use without fatigue or cracking.

The critical buckling load of 84.98 kN obtained in the buckling analysis is significantly higher than the design loads. The critical stress of 69.09 MPa further shows that the structure can maintain stability under load. The Johnson method was deemed valid based on the column's length and moment of inertia.

The shaft calculations also supported the rigidity of the system. Force and moment analyses in both x and y axes revealed a maximum stress of 4.52 MPa at the shaft's most stressed point, which remains well below the material's yield strength. This confirms that no structural weakness exists in the shaft. Its resistance to bending and shear combinations reinforces the mechanical durability of the device.

Subsequent to theoretical calculations, ANSYS simulations showed maximum von Mises values of 487.97 MPa for U-type and 522.9 MPa for V-type bending. Although the discrepancy is not extreme, the reason for the deviation from theoretical values is believed to be the displacement-based loading method used, which does not apply a linear force. Springback values were found to be 1.9° through the use of the 'part transform' command in ANSYS Mechanical, which is very close to the 1.82° theoretical result.

All these evaluations confirm the consistency between theoretical analysis and numerical simulations, showing that the developed manual press brake has been designed in accordance with sound engineering principles. The system offers a successful combination of strength, stability, precision, and user ergonomics. The obtained data indicates that the device can be used reliably in industrial applications. This study not only developed a prototype but also completed a comprehensive design process supported by engineering calculations, material selection, and validation tests. As a result, the device has met all targeted performance criteria in both academic and practical contexts and lays a solid foundation for future improvements.

## **7. REFERENCES**

- 1- Serope Kalpakjian, Steven Schmid - Manufacturing Engineering & Technology
- 2- Mikell P. Groover - Fundamentals of Modern Manufacturing\_ Materials, Processes, and Systems
- 3- Kurt Lange - Handbook of Metal Forming
- 4- Jack Hu, Zdzislaw Marciniak, John Duncan - Mechanics of Sheet Metal Forming
- 5- Taylan Altan and Erman Tekkaya - Sheet Metal Forming Processes and Applications
- 6-(Hibbeler, R. C. (2017). Mechanics of Materials (10th Edition). Pearson Education.
- 7-Gere, J. M., & Goodno, B. J. (2012). Mechanics of Materials (8th Edition). Cengage Learning.
- 8-Beer, F. P., Johnston, E. R., DeWolf, J. T., & Mazurek, D. F. (2014). Mechanics of Materials (7th Edition). McGraw-Hill Education.)
- 9-T.H.G. Megson - Structural and Stress Analysis (2019, Butterworth-Heinemann)
- 10-E. Paul DeGarmo, J T. Black, Ronald A. Kohser - DeGarmo's Materials and Processes in Manufacturing (2007, Wiley)
- 11-Ivana Suchy - Handbook of Die Design (2005, McGraw-Hill Professional)
- 12- Materials & Design 2002-apr vol. 23 iss. 2 Volkan Esat\_ Haluk Darendeliler\_ Mustafa Ilhan Gokler - Finite element analysis of springback in bending of aluminium sheets (2002)
- 13-Serope Kalpakjian and Steven R. Schmid - Manufacturing Processes for Engineering Materials (2014, Pearson Education)
- 14.Benson, S. D. (1997). Press Brake Technology: A Guide to Precision Sheet Metal Bending. Society of Manufacturing Engineers (SME)
- 15.Budynas, Nisbett. (2015). SHIGLEY'S MECHANICAL ENGINEERING DESIGN. McGraw-Hill Education.
- 16-<https://www.scribd.com/presentation/23678731C0/Transmitted-Load>
- 17-[https://www.engineeringtoolbox.com/angular-velocity-acceleration-power-torque-d\\_1397.html?utm\\_source](https://www.engineeringtoolbox.com/angular-velocity-acceleration-power-torque-d_1397.html?utm_source)
- 18-[https://khkgears.net/new/gear\\_knowledge/gear\\_technical\\_reference/gear\\_forces.html](https://khkgears.net/new/gear_knowledge/gear_technical_reference/gear_forces.html)
- 19-Bhandari. (2010). Design of Machine Elements. McGraw-Hill Education.

20-ANSI/AGMA 2001-D04

21-<https://www.fushunspecialsteel.com/aisi-4140-alloy-steel/>

22-[https://www.kisssoft.com/en/products/publications/brochures/reliability-lifetime-and-safety-factors?utm\\_source=chatgpt.com](https://www.kisssoft.com/en/products/publications/brochures/reliability-lifetime-and-safety-factors?utm_source=chatgpt.com)

23-<https://www.mdpi.com/2075-4701/13/3/587#>

24-Kalpakjian S., Schmid S.R. Manufacturing Engineering and Technology. Fourth Ed. 2001. Prentice Hall.